STUDY OF SUBMERGED ARC WELDING OF MILD STEEL WITH IRON POWDER MIXED FLUX

A DISSERTATION

SUBMITTED IN PARTIAL FULFILLMENT OF THE REQUIREMENTS
FOR THE AWARD OF THE DEGREE

OF

MASTER OF TECHNOLOGY

IN

[**PRODUCTION ENGINEERING**]

Submitted by:

[**PARAS GUPTA**]

(**Roll No. 2K16/PIE/003**)

Under the supervision

of

Dr. M. S. NIRANJAN

(Assistant Professor)

DEPARTMENT OF MECHANICAL ENGINEERING

DELHI TECHNOLOGICAL UNIVERSITY

(Formerly Delhi College of Engineering)

Bawana Road, Delhi-110042

CANDIDATE'S DECLARATION

I, PARAS GUPTA, 2K16/PIE/003 student of M.Tech, PRODUCTION ENGINEERING hereby declare that the project Dissertation titled "**STUDY OF SUBMERGED ARC WELDING OF MILD STEEL WITH IRON POWDER MIXED FLUX**", which is submitted to the **Department of MECHANICAL ENGINEERING**, Delhi Technological University, Delhi in partial fulfilment of the requirement for the award of degree of Master of Technology, is original and not copied from any source without proper citation. This work has not previously formed the basis for the award of any Degree, Diploma Associate ship, Fellowship or other similar title or recognition.

Place: Delhi

Date:

PARAS GUPTA

2K16/PIE/003

CERTIFICATE

I herby certify that the Project Dissertation entitled "**STUDY OF SUBMERGED ARC WELDING OF MILD STEEL WITH IRON POWDER MIXED FLUX**", which is submitted by **Mr. PARAS GUPTA**, **2K16/PIE/003, Mechanical Engineering,** Delhi Technological University, Delhi in partial fulfilment of the requirement for the award of the degree of Master of Technology, is a record of the project work carried out by the student under my supervision. To the best of my knowledge this work has not been submitted in part or full for any Degree or Diploma to this university or elsewhere.

Place: Delhi

Supervisor

Date:

Dr. M. S. Niranjan

(Assistant Professor)

ACKNOWLEDGEMENT

ABSTRACT

Submerged Arc Welding (SAW) is the most widely utilized for joining of thick segments welding like in thick sections. The submerged arc welding gives the high metal deposition rate, having capacity to weld thick areas with longer weld running with proficiently.

The design of experiment (DOE) with 3 factors such as arc voltage, travel speed, and %age of iron powder and 5 levels with rotatable Central Composite Design have been used to develop the experimental plan. Response Surface Methodology (RSM) was utilized to build up the numerical models co-relating the process parameters with the reasponses such as bead geometry (bead width, bead height, and depth of penetration) and residual stresses. The models once created were checked for sufficiency utilizing analysis of varience (ANOVA). From the adequate models the significant terms were chosen utilizing p test. Fundamental and communication impacts of the process parameters on weld bead geometry and residual stresses are displayed in graphical form. The created models can be utilized to forecast the imperative weld bead measurements and control of the weld bead quality by choosing appropriate process parameters values.

After performing the experiments, various outcomes are analysed by using RSM. It has been observed that the bead width increases with the increase of voltage, while the change in other two parameters is less. The increase in %age iron powder increases all three bead geometry parameters but increase in penetration is more than the other two bead parameters. Travel speed is most sensitive parameter to all three bead parameter; but depth of penetration is more sensitive towards travel speed.

It has also been observed that %age of iron powder, Arc voltage, and welding speed have a significant effect on the residual stress. The welding speed greatly increased the residual stresses over the whole selected input levels (42 – 46 cpm). Whereas, arc voltage has an adverse effect, and the residual stresses value decreased largely at high level (37 Volt).

Key words: SAW, DOE, RSM, Bead Geometry, Residual stress and Weld Metallurgy.

TABLE OF CONTENTS

CHAPTER 4 EXPERIMENTATION

CHAPTE 5 STATISTICAL ANALYSIS

LIST OF FIGURES

LIST OF TABLES

LIST OF SYMBOLS

Symbol Represents units:

P: Bead Penetration (mm)

W: Bead Width (mm)

H: Bead Height (mm)

V: Voltage (Volts)

A: Current (Ampere)

S: Travel Speed (mm/min)

N: Nozzle-to-plate-distance (mm)

ABBREVIATIONS

CCD: Central Composite Design

RSM: Response Surface Methodology

ANN: Artificial Neural Network

HAZ: Heat Affected Zone

CHAPTER 1

INTRODUCTION

1.1 Introduction

Submerged Arc Welding (SAW) is normally utilized metal joining process in the industrial application, particularly suited for joining of thick and substantial heavy sections. The nature of any weld procedure is described by the weld distortion after completion, mechanical properties and weld bead geometry. Out of these components, the weld bead geometry is the simplest to gauge and control. In this way by controlling the weld bead geometry, we can effectively control the weld quality. The relationship between the process factors and the weld bead geometry is exceptionally intricate and requires a scientific way to deal with evaluate the connection between them.

Aside from impacting the bead geometry, the input process parameters likewise influence the metallurgical parts of the metal being joined. The smaller scale hardness, the unique stages constituting the smaller scale structure, the level of various stages, grain estimate and so forth are to a great extent impacted by the info procedure factors and at last they influence the execution of the welded metal in various applications.

In submerged arc welding a granular weld flux layer protects the welding point from the influence of the surrounding atmosphere. Unused flux can be extracted from behind the welding head and subsequently recycled. The filler material is an uncoated, continuous wire electrode, applied to the joint together with a flow of grained flux, which is supplied from a flux hopper through a tube. The electrical resistance of the electrode should be as low as possible to facilitate welding at a high current, and so the welding current is supplied to the electrode through contacts very close to the arc and immediately above it. The current can be direct current with electrode positive (reverse polarity), with negative (straight polarity), or alternating current. The arc burns in a cavity which, apart from the arc itself, is filled

with gas and metal vapour. The size of the cavity in front of the arc is delineated by un-melted basic material and behind it by the molten weld.

Welding is a fabrication process that joins two metals or non-metals by producing joint between them. This is generally achieved by heating the specimen up to their melting temperature with or without the addition of filler materials, to form a pool of molten metal that cool and solidifies to become a strong joint. While often an industrial process, welding can be done in many different environments, including open air, under water and in outer space.

With the advent of newer materials, precise performance and quality requirements in the industry, engineers became increasingly aware of the weld quality. The major factors which decide the quality of a joint are mechanical properties of the welded joint, distortion of the welded structure and the bead geometry features. The studies of the effects of various welding process parameters on the formation of bead and bead geometry have attracted the attention of many researchers to carry out further investigations. Design of experiment (DOE) combined with Response surface methodology (RSM) is a powerful statistical tool to determine and represent the cause and effect relationship between responses and input control variables influencing the responses as a two or three dimensional hyper surface.

The mechanical performance and application of any welded joint is affected by the metallurgical properties of the welded joints. Over the years researchers have carried out investigations to understand the metallurgical changes taking place during the welding and to co-relate these changes with the welding process variables. The present literature review has been carried out in the areas concerning the influence of input process variables in the bead geometry, application of RSM to develop mathematical models to model the relationships between the inputs and the outputs of a process.

Chapter 2
LITERATURE REVIEW

2.1 Influence of Input Process Variables on the Bead Geometry

R.S. Chandel [1] presented theoretical predictions of the effect of current, electrode polarity, electrode diameter and electrode extension on the melting rate, bead height, bead width and weld penetration, in submerged-arc welding. They studied that the melting rate of SAW can be increased by four methods: (i) using higher current; (ii) using straight polarity; (iii) using a smaller diameter electrode; and (iv) using a longer electrode extension. The percentage difference in melting rate, bead height, bead width, and bead penetration is affected by the current level and polarity. When a smaller diameter electrode is used, the increase in the current level does not make much difference to the percentage change in bead height, bead width, and weld penetration.

Erdal Karadeniz et al [2] in their study, the effects of various welding parameters on welding penetration in Erdemir 6842 steel having 2.5 mm thickness welded by robotic gas metal arc welding were investigated. The welding current, arc voltage and welding speed were chosen as variable parameters. The depths of penetration were measured for each specimen after the welding operations and the effects of these parameters on penetration were researched. The welding currents were chosen as 95, 105, 115 A, arc voltages were chosen as 22, 24, and 26 V and the welding speeds were chosen as 40, 60 and 80 cm/min for all experiments. As a result of this study, it was found that increasing welding current increased the depth of penetration. In addition, arc voltage is another parameter in incrimination of penetration. However, its effect is not as much as current's. The highest penetration was observed in 60 cm/min welding current.

Gunaraj and Murugan [3] have highlighted the use of RSM to develop mathematical models and plot contour graphs relating important input parameters namely the open-circuit voltage, wire feed-rate, welding speed and nozzle- to-plate distance to some responses namely, the penetration, reinforcement, width and percentage dilution of the weld bead in SAW of pipes. They demonstrated that all

responses decrease with increasing welding speed. Also, when the nozzle-to-plate distance increases all responses decrease, but reinforcement increases. Moreover, an increase in the wire feed-rate results in an increase in all responses but the width remains unchanged.

In 1999, Gunaraj and Murugan [4] also studied the effect of SAW parameters on the heat input and the area of HAZ for low-carbon steel with two joint types, bead-on- plate and bead-on-joint, using mathematical models developed by RSM. They found that for the same heat input, the area of the HAZ is greater for the bead-on-plate than that for bead-on-joint. They found that the effect of SAW parameters on the area of HAZ in both cases follows the same trend.

Yang et al [5] have used linear-regression equations for computing the weld features (melting rates, total fusion area, penetration, deposit area, bead height and bead width) from SAW process variables (electrode extensions range, welding voltage, welding current, welding speed and electrode diameter) using both positive and negative electrode polarity. The base material was a 19 mm thick ASTM A36 steel plate. They managed to develop regression equations for each weld feature in both polarity conditions. Their results indicated that the linear-regression equations were equally useful for computing the various features of the SAW process.

Bipin Kr, Srivastav et al [6] reviewed the effects of arc welding parameters on mechanical properties of ferrous metals/alloys. Their study of the various works, review that, the selection of the suitable process parameters are the primary means by which acceptable heat affected zone properties, optimized bead geometry and minimum residual stresses are created. Some researchers realized that the mechanical properties of weld are influenced by the composition of the base metal and to a large extent by the weld bead geometry and shape relationship as well. Some of the researchers observed that with increase in electrode stick out, hardness of the weldment increases, yield strength and impact value decreases, ultimate tensile strength of the joint initially decreases but thereafter increases provided welding current and voltage are kept at constant levels.

From the discussion on the above-mentioned literature it is observed that in different welding processes the weld bead parameters such as penetration, bead width, reinforcement height etc. are largely influenced by various welding parameters such as arc current, voltage, and travelling speed. In SAW the main factors affecting the bead geometry are arc voltage, current, travel speed, and nozzle

plate distance.

2.2 Application of CCD matrix and regression analysis for designing the experiments and developing the mathematical model

It consists of the following steps:

➢ Designing of a set of experiment for adequate and reliable measurement of the true mean response of interest.

➢ Determination of mathematical model with best fits

➢ Representing the direct and interactive effects of process variables on the best parameters through two dimensional and three dimensional graphs.

Benyounis et al [7] have proposed models using RSM to investigate the effect of welding parameters in SAW (welding current, arc voltage and welding speed) on the impact strength at two testing temperatures of 50 ^{0}C and 27 ^{0}C. The aim was to predict and optimize the impact strength of the spiral-welded joints with respect to the process parameters. It was observed that the welding current was the most significant factor associated with the impact strength, then the welding speed, whereas the welding voltage has no significant effect within the factors domain investigated. They listed the optimal welding conditions that would lead to acceptable impact strength with improving the process productivity.

Murugan and Gunaraj [8] used 5 level 4 factor central composite rotatable design matrix for Prediction and control of weld bead geometry and shape relationships in submerged arc welding of pipes. Arc voltage, wire feed rate; welding speed and nozzle-to-plate distance were considered as the main factors affecting the bead Geometry. Mathematical models have been developed for SAW of pipes using five level factorial techniques to predict three critical dimensions of the weld bead geometry and shape relationships. The models developed have been checked for their adequacy and significance by using the *F*-test and the *t*-test, respectively. Out of the four process variables considered, wire feed rate had a significant positive effect but welding speed had an appreciable negative effect on most of the important bead parameters. Penetration increased by about 1.3mm as wire feed rate was increased from −2 to +2 limit whereas penetration decreased by about 1mm as welding speed was increased from −2 to +2 limit. Arc voltage had a less significant negative effect on penetration and reinforcement but had a positive effect on bead

width, penetration size factor and reinforcement form factor. As wire feed rate had a positive effect but welding speed had a negative effect on most of the bead parameters, the interaction effects of wire feed and travel speed were similar for most of the parameters. Penetration, width, penetration size factor and reinforcement form factor all increased with the increase in wire feed rate for all values of welding speed but this increasing rate of the bead parameters with the increase in wire feed rate is gradually decreased with the increase in travel speed.

Koleva [9] has carried out another work by applying RSM to establish the relationship between performance characteristics (weld-depth, weld-width and thermal efficiency) and its influencing factors (beam power, welding velocity, focus position, focusing current of the beam and the distance to the sample surface) for EBW of austenitic stainless steel. Optimal welding regimes were found through the thermal efficiency optimization. New statistical approaches were proposed to choose the focus position at a condition of maximum thermal efficiency and welding depth.

Benyounis et al [10] have applied RSM to investigate the effect of laser welding parameters (laser power, welding speed and focal point position) based on four responses (heat input, penetration, bead width and width of HAZ) in CO_2 laser butt-welding of medium carbon steel plates of 5 mm thick. They found that the heat input plays an imported rule in the weld-bead parameters; welding speed has a negative effect while laser power has a positive effect on all the responses.

Heiderzadeh et al [11] applied RSM for his investigations of the tensile behavior of friction stir welded AA 6061-T4 aluminum alloy joints. In this investigation response surface methodology based on a central composite rotatable design with three parameters, five levels and 20 runs, was used to develop a mathematical model predicting the tensile properties of friction stir welded AA 6061-T4 aluminum alloy joints at 95% confidence level. The three welding parameters considered were tool rotational speed, welding speed and axial force. Analysis of variance was applied to validate the predicted model. Microstructure characterization and fractography of joints were examined using optical and scanning electron microscopes. Also, the effects of the welding parameters on tensile properties of friction stir welded joints were analyzed in detail. The results showed that the optimum parameters to get a

maximum of tensile strength were 920 rev/min, 78 mm/min and 7.2 KN, where the maximum of tensile elongation was obtained at 1300 rev/min, 60 mm/min and 8 KN. The literature review has brought about an understanding of the use of regression analysis to determine and represent the cause and effect relationship between true mean response and input control variables influencing the response as a two or three dimensional hyper surface.

Anderson et al [12] in 1990 pioneered the use of artificial neural networks for the modeling of an arc welding process. In their paper Artificial neural networks were studied to determine their applicability to modeling and control of physical processes. Some basic concepts relating to neural networks and how they can be used to model weld-bead geometry in terms of the equipment parameters selected to produce the weld were explained. Approaches to utilizing neural networks in process control are discussed. The need for modeling transient as well as static characteristics of physical systems for closed-loop control is pointed out, and an approach to achieve this is presented. The performance of neural networks for modeling is evaluated using actual welding data. It was concluded that the accuracy of neural network modeling is fully comparable with the accuracy achieved by more traditional modeling schemes.

George E. Cook et al. [13] evaluated artificial neural networks for monitoring and control of the Variable Polarity Plasma Arc Welding process. Three areas of welding Application were investigated: weld process modeling, weld process control, and weld bead profile analysis for quality control.

D.S. Nagesh, G.L. Datta [14] in their work used artificial neural networks to model the shielded metal-arc welding process. Back-propagation neural networks are used to associate the welding process variables with the features of the bead geometry and penetration. These networks have achieved good agreement with the training data and have yielded satisfactory generalization. A neural network could be effectively implemented for estimating the weld bead and penetration geometric parameters. The results of these experiments show a small error percentage difference between the estimated and experimental values.

Sukhomay pal et al [15] used ANN for modeling of weld joint strength prediction of pulsed MIG using arcs signals. Their paper addressed the weld joint strength monitoring in pulsed metal inert gas welding (PMIGW) process. Response surface methodology was applied to perform welding experiments. A series of experiments were carried out by applying response surface method.. A multilayer neural network model was developed to predict the ultimate tensile stress (UTS) of welded plates. Six process parameters, namely pulse voltage, back-ground voltage, pulse duration, pulse frequency, wire feed rate and the welding speed, and the two measurements, namely root mean square (RMS) values of welding current and voltage, were used as input variables of the model and the UTS of the welded plate is considered as the output variable. The obtained experimental data was used to train and test ANN model of various architectures; and 8-13-18-1 architecture with learning rate and momentum coefficient of 0.9 and 0.35, respectively, was found as the best one for the current purpose. A multiple regression model was also developed and its performance was compared with the performance of the ANN model. It was found that the error in prediction of weld strength from the neural network model is less than that from the regression model.

The study of Abdulkadir C`evik et al [16] presented use of neural network (NN) for the prediction of ultimate capacity of arc spot welding. The proposed NN model is based on experimental results. The ultimate capacity of arc spot welding is modeled in terms of weld strength, average welding thickness and diameter. The results of the proposed NN model are later compared with results of existing codes and are found to more accurate. Parametric studies are also carried out to analyze the effect of each variable.

2.3   Influence of process variables on the metallurgy of the welded specimen

The metallurgy of the base metal plays a major role in deciding the mechanical properties and application of the base metal. Research work has been carried out to co-relate the metallurgical changes with the input process variables and thus, to control the metallurgy of the welded specimen.

M. Eroglu et al [17] carried out investigations to study the effect of coarse initial grain size on microstructure and mechanical properties of weld metal and HAZ of low carbon steel. In this study, the effects of coarse initial grain size with

varying heat inputs on microstructure and mechanical properties of weld metal and heat-affected zone (HAZ) were investigated. The original and grain-coarsened specimens were welded using a submerged arc welding machine with heat inputs of 0.5, 1 and 2 kJ/mm. Following the welding, microstructure, hardness and toughness of weld metals and HAZs were investigated. From the results, they tried to establish a relationship between initial grain size, microstructure, hardness and toughness of weld metals and HAZs. Considering the heat input, it was observed that the coarse initial grain size had a great influence on the microstructure, hardness and toughness of HAZ of low carbon steel. Thus, taking into consideration the plate thickness, a higher heat input should be used with respect to the maximum toughness of the HAZ in the welding of grain-coarsened low carbon steels.

D.V.Kiran et al [18] investigated the influence of process variables on weld bead quality in 2 wire tandem submerged arc welding of HSLA steel. In particular, the quantitative effects of the trailing wire current pulses and negative current pulse duration, leading wire current, and welding speed on the weld bead dimensions and mechanical properties are studied at fifty different sets of welding conditions that are designed following the principle of two-level, f.ive factor central composite rotatable design. The experimental results show that the final weld bead width and reinforcement height are primarily influenced by the trailing wire current while the penetration is influenced by the leading wire current with the other conditions remaining constant. Increase in welding speed tends to reduce weld pool size leading to higher cooling rate that encourages greater volume fraction of acicular ferrite phase and better weld bead mechanical properties. The predictions of weld dimensions and mechanical properties from the empirical relations, which are developed based on the experimental results, are in fair agreement with the corresponding measured values within the ranges of the welding conditions considered in the work.

Gunaraj et al [19] developed mathematical models for prediction and comparison of area of the heat-affected zone for the bead-on-plate and bead-on-joint in submerged arc welding of pipes. The amount of heat input to the weld metal increases as voltage or wire feed rate or both increase. The heat input decreases with increase in travel speed. They found that voltage and wire feed rate had a positive effect on area of HAZ while travel speed and nozzle-to-plate distance had a negative

effect. For the same heat input the area of HAZ is greater on the plate tan on the joint. The direct and indirect effects of process variables on the area of the HAZ on both the bead-on-plate and the bead-on-joint are found to be the same. It is also found that the slopes of the individual plots are generally equal.

Kolhe et al [20] carried out a detailed work in prediction of microstructure and mechanical properties of multi pass SAW. A detailed study on the microstructure, phase analysis and mechanical properties, HAZ width of SA weld metal multi pass joint and heat-affected zone of 16mm thick mild steel plate was carried out. The various sub-zones in the microstructure were observed in the HAZ of SA weld are spheroidized, partially transformed, grain refined and grain coarsened. Welding heat input can control the percentage of phases in the welded structures. More variations in bulk hardness of the fractured samples were observed than welded samples. More HAZ width at top region of welded specimen was seen than that of bottom region. For increase in heat input the percentage of graphitic phase was slightly decreased whereas the percentage of ferrite sharply increased and finally the ferritic structures were observed. The proportionate value of micro hardness was observed for low heat input whereas for increased heat input variations in hardness value was observed.

Amit kumar [21] carried out detailed work on metal powder by adding Nickel powder in SAW flux and apply taguchi methodology with 5 levels and see the effects of metal powder on bead geometry. The current work is an effort to study the effect of Nickel metal powder addition in flux, on the impact strength, bead height and bead width, of IS 2062 steel during submerged arc welding. The effect of Nickel metal powder addition on fluxes by keeping the welding parameters like welding voltage and welding speed constant has been evaluated. Taguchi technique has been used for the design of experiments. The effects of flux, voltage and travel speed have been evaluated on the impact strength, bead height and bead width. The effect of all the input parameters on the output responses have been analyzed using the analysis of variance (ANOVA).

2.4 Research gap:

- To prepare the samples of mild steel with dimensions 260x65x12 mm.
- To prepare the granular flux by adding the appropriate quantity of iron powder in the existing flux.
- To study the effects of various parameters such as Arc voltage, Travel speed and iron powder on the response like weld bead geometry and residual stress using response surface methodology.
- To study the microstructure of the samples with the use of optical microscope.

2.5 Research Objectives:

Based on the literature survey, the following research objectives have been drawn.

1. To prepare the samples of mild steel with dimensions 260x65x12 mm.
2. To prepare the granular flux by adding the appropriate quantity of iron powder in the existing flux.
3. To study the effects of various parameters such as Arc voltage, Travel speed and iron powder on the response like weld bead geometry and residual stress using response surface methodology.
4. To study the microstructure of the samples with the use of optical microscope.

CHAPTER 3

PROBLEM DESCRIPTION

3.1 Introduction:

SAW comes into picture in 1935. In this process the molten metal and arc covered with the granulated slag combination of calcium oxide, silica, manganese oxide and some other compounds. This layer of slag also protects worker from ultraviolet rays and fumes which are generally produces in saw welding process and enhances the efficiency of heat transfer.
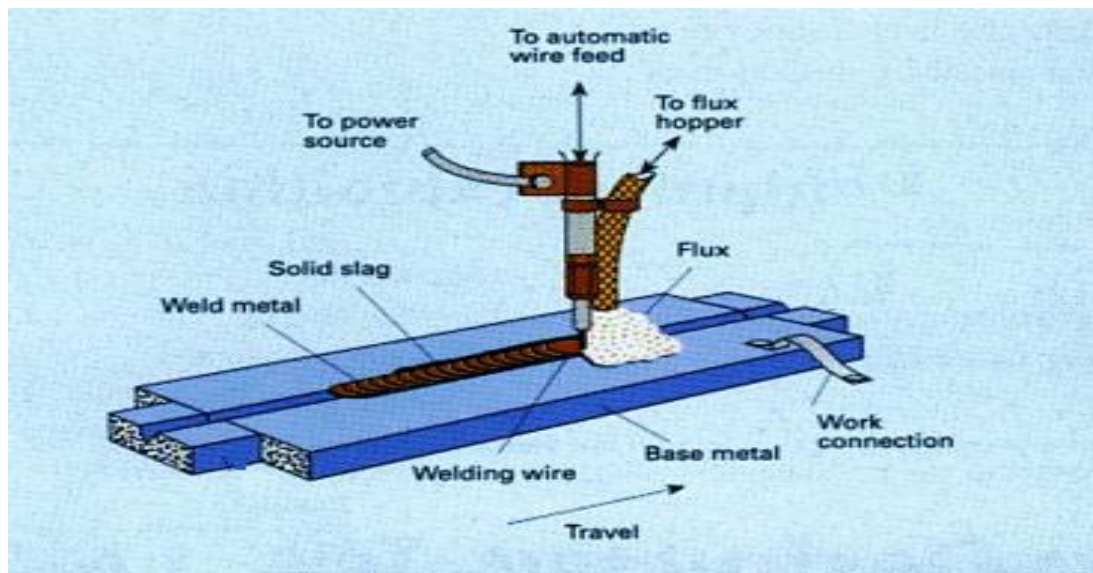
Figure 3.1: schematic view of the saw process [3]

SAW is mostly used to join the materials which are having more thickness. Schematic of submerged arc welding process is shown in fig. 3.1. SAW is generally a automatic welding process but it may be semiautomatic. The welding flux also added in two ways one is gravity feed and another one pressurised flux feeding for this purpose a hopper is used which is fixed at head of the welding and a tubular section connected with hopper for spreading the flux continuously ahead of arc. The SAW generally used for flat position and horizontally but in horizontal position we required some special arrangement to hold the slag. Current varies in SAW is generally varies from 300-2000 A it may also goes up to 5000 A. Source of power

can be DC or AC for single pass or it can combination of both for multi pass welding.

The quality of weld also be dependent on workers experience because at the time of welding we cannot see the weld pool. After the process un-melted slag can be reclaimed for the purpose of reusing. There are some slag which form on weld bead can detach with the help of hammer but most of the time it will be detach automatically after 5-6 seconds of welding. As we know the efficiency of manual arc welding generally less because there is more heat taken by atmospheric air but this not happens in saw because arc is protected by flux then we got efficiency up to 60%. The SAW is automatic process subsequently accuracy can also be enhanced because less human invention will be there and we can additionally said that SAW is worker friendly process because there is spatter and there is less fumes during the process.
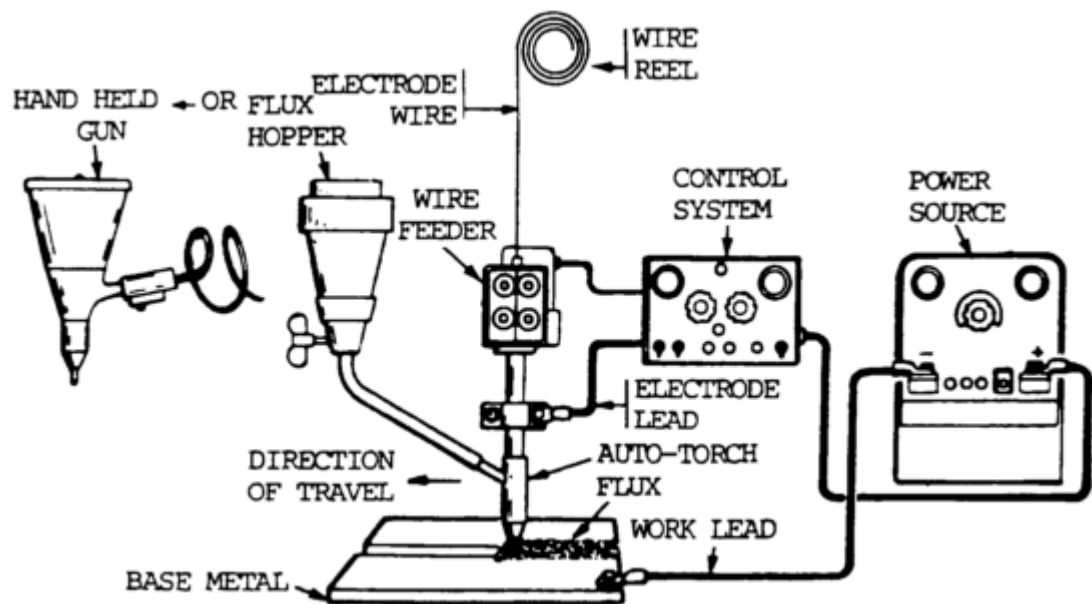
3.2 SAW equipment:

Figure 3.2 SAW machine in operation [41]

The figure 3.2 shows the basic equipments of SAW process. Main elements of a semi automatic SAW welding are a wire feeder, control system and power source.

3.3 Process Factors:

13

Since the operator can't see the bead while the welding is in advance it is important that the parameters must be set with incredible precision. Every one of the factors has a specific impact upon the geometry of weld bead and material deposition rate of weld material. It is exceptionally basic to set a few factors to amend extend before beginning SAW for accomplishing great quality welds. Following are the Procedure factors in Observed:

- Travel speed
- Welding current
- Rate of heat input
- Electrode size
- Electrode stick out

3.4 Welding current:

It controls the liquefying ability of the electrode and in this manner the deposition rate. It additionally controls the penetration. Too high a current causes excessive weld reinforcement, which is inefficient, and consume in the event of thinner plates or in badly fitted joints, which are not appropriately backed.

3.5 Arc voltage:

The outcome of arc voltage is seen on arc length in direct proportion. Heat availability will increases by increasing arc length because voltage will be increasing. However if we increases arc length generally the arc will spread more and bead width is more also penetration will observe less in that case. If we talk about flux so in this case flux required more because by getting more heat flux will melt more.

3.6 Travel speed:

If fix welding parameters like current and voltage by decreasing the weld speed we observe that penetration, bead width and fusion will be increases on the other side if we increases speed then we see the opposite effect. In all the cases we required to maintain a optimum welding speed because speed is more then it produces undercut like defects and if speed is less then it produces more the deposition on the weld joint.

3.7 Size of electrode:

The size of electrode directly affects the current density. Generally wire of 2-5 mm diameter uses for proper penetration and proper bead width although it also depends on the material thickness to be welded.

3.8 Heat input rate:

The current and voltage are related with heat input rate in direct proportion and inversely with welding speed.

HIR= V*I/S

Where, HIR= heat input rate

V   = arc voltage (volt)

I   = welding current (amp)

S   = weld speed (mm/sec)

Heat input rate related to heat affect zone, thickness of the weld joint and the cooling rate of weld metal. By increasing the heat rate some increment in these parameters and vice versa. We can get a good microstructure for a particular application if heat rate is appropriate. High cooling rate along with high heat rate gives a good hardness to the joint.

3.9 Nomenclature of weld bead:

The mechanical properties of weld bead can be altered by the bead geometry and this weld geometry can be changed by various weld parameters like weld current, arc voltage, travel speed and changing the composition of flux material. The weld bead specification done by reinforcement height, bead width, area of reinforcement, height of penetration, area of penetration and the angle made by weld bead with the top of the base plate.
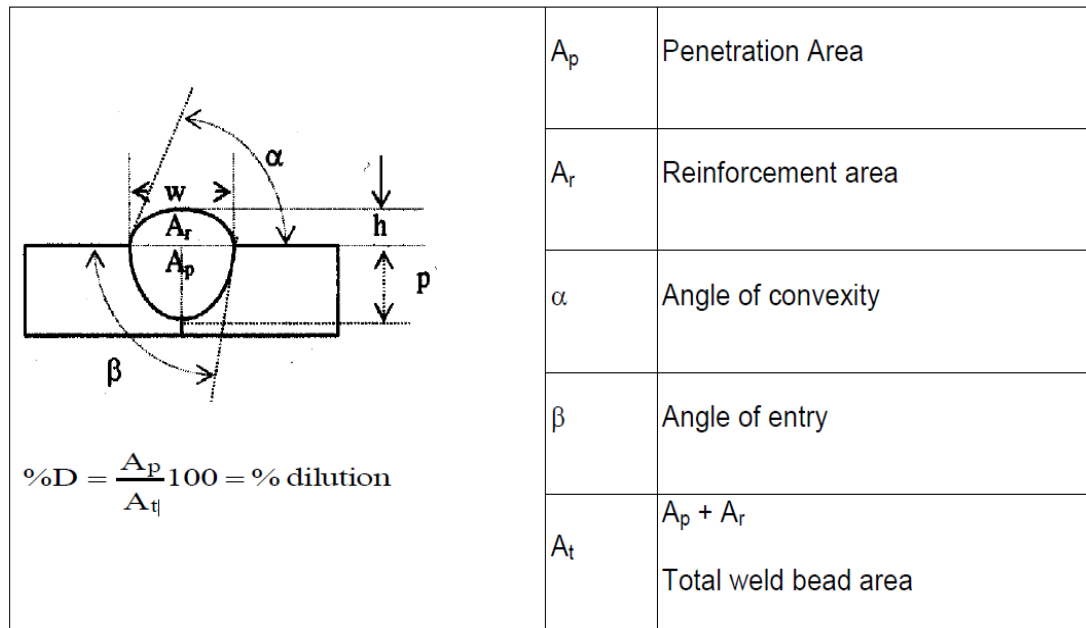
A_p	Penetration Area
A_r	Reinforcement area
α	Angle of convexity
β	Angle of entry
A_t	$A_p + A_r$ Total weld bead area

$$\%D = \frac{A_p}{A_t}\,100 = \%\ \text{dilution}$$

Figure 3.3: weld bead geometry [20]

3.9.1 Bead width: The bead width can be defined as the maximum width of the weld metal deposited. By increasing arc voltage, arc current and electrode weaving, width of weld bead increases and by increasing welding speed the bead width deceases.

3.9.2 Penetration height: The separation between the highest points of the base plate to the maximum depth of the weld nugget is measures as penetration height.

3.9.3 Penetration area: load varying capacity is defined by the penetration area. Penetration area affects the weld strength and it is defined the area of the fusion zone below the upper plane of the base plate.

3.9.4 Reinforcement height: it can be characterized as the greatest range from the highest point of the metal saved to the highest point of the base plate.

3.9.5 Reinforcement area: reinforcement area is the area of deposited metal above the top of the plate.

3.10 SAW Wire

There variation can be done in terms of wire ie; single wire, double wire, triple wire, single wire with hot wire addition and single wire with metal powder addition. All factors are contributed in improving the efficiency and rate of metal deposited.

3.11 Fluxes in SAW:

Fluxes help to make sound welds and also they make welding easier by making the blanket on the weld area of the chemical compound in the form of flux. Many of the metals during welding process react with atmospheric process so the fluxes are also used to prevent hazardous effect of environmental gasses. Their are deep study will be required for proper flux which are compatible with electrode wire and the material which to be welded because all these things will alter the mechanical properties and also surface appearance.

3.12 Properties of SAW flux:

1. It should be good arc initiator and also give a stable arc.
2. The flux is in the granular form so that their flow will be smooth in the tube with a desired flow rate.
3. It should form slag in the form of CaO, MgO etc. This will protect weld zone from atmospheric oxygen.
4. It must not produce any harmful gases by the time of increasing temperature of weld zone.

3.13 Classification of flux:

The weld bead properties largely depend on how the fluxes are manufactured. The classification is basically two types,

3.13.1 Based on mechanical mixing:

1. Fused flux: The various are melted in an electric arc furnace. When it will produce a glossy shape paste then it will be cooled , crushed and then it will be grounding after that homogeneous grains will be taken out by sieving action, generally their size vary in-between 0.2-1.2 mm.
2. Agglomerated flux: agglomerated fluxes are generally heterogeneous nature because it will be made up of powders. The various powders mixes with a suitable binding agent like water glass then it will be dry in the furnace to 700-800 degree centigrade and then take out required grain size by sieving action.

3.13.2 Based on chemical composition:

The flux can be differentiating on the basis of basicity and acidity. If flux having higher basicity then it gives better impact values, but on the another side it reduces welding speed and creates fine rippling of weld bead because of this reason we required an optimum amount of basicity.

3.14 Advantages and limitations of SAW:

3.14.1 Advantages of submerged arc welding:

1. It gives deep penetration.
2. Gives sound welding (because less atmospheric gasses come into contact with molten pool).
3. Gives high deposition rate (nearly 40kg/h).
4. This welding process is suitable for indoor as well as outdoor.
5. Flux can be recovered very efficiently. (Nearly 60-80%).
6. The loss of heat is very less because arc always covered with flux as a blanket.
7. Operator friendly because less fumes or light is emitted.
8. The joint is corrosion resistant, ductile and also less distortion in the joint is reported.

3.14.2 Limitation of submerged arc welding:

1. For multi pass welding requires post weld slag removal.
2. Environmental problem like used flux and slag residue creates health and safety concern.
3. Flux handling system is difficult comparatively.
4. The positions of welding are limited to flat and horizontal positions.
5. Only used for ferrous metals and some nickel based alloy.

3.15 Applications of SAW:

SAW is mostly used for longitudinal joint because due to loose granular flux and high fluidity of weld pool it creates some problem in other joint. For circumferential arrangement the work piece rotated on a fix weld head so that the welding taking place in flat position. One interesting fact about SAW is that there is no limitation of the weld thickness for that we can adopt multi pass also. The process mostly used to

join low alloy steel and stainless steel although it is also capable to join non-metals if a proper feed wire and flux combination used. Following are the industries where SAW used,

- SAW is most suitable for ship industries because long run weld in flat position SAW can be efficiently work.
- Earthmoving equipments and manufacturing of pressure vessels
- Storage tank and structural assembly, structure of railway coaches, fabrication of penstocks.

3.16 Response Surface Methodology (RSM)

3.16.1 Introduction

The Response Surface Methodology (RSM) is a collection of mathematical and statistical techniques useful for the modelling and analysis of problems in which a response of interest is influenced by several variables and the objective is to optimize this response. The most extensive application of RSM is particularly in situations where several input variables potentially influence some performance measure or quality characteristic of the product or process. This performance measure or quality characteristic is called Response. It is typically measured on continuous scale. Most of the real world application of RSM will involve more than one response. The input variables are sometimes called independent variables and they are subject to the control of the engineer or scientist, at least for the purpose of a test or an experiment. In most RSM problems, the true response function f is unknown. In order to develop a proper approximation for f, the experiments usually starts with a low-order polynomial in some small region. If the response can be defined by a linear function of independent variables, then the approximating function is a first-order model. A first-order model with 2 independent variables can be expressed as

$$Y = b_0 + b_1 x_1 + b_2 x_2 + e$$

If there is a curvature in the response surface, then a higher degree polynomial should be used. The approximating function with 2 variables is called a second-order model:

$$Y = b_0 + b_1 + b_2 + b_{11}.x^2_{11} + b_{22}.x^2_{22} + b_{12}.x_{12} + e$$

In general all RSM problems use either one or the mixture of the both of these models. In order to get the most efficient result in the approximation of polynomials the proper experimental design must be used to collect data. Once the data are

collected, the Method of Least Square is used to estimate the parameters in the polynomials. The response surface analysis is performed by using the fitted surface. The response surface designs are types of designs for fitting response surface.

3.16.2 Central Composite Design

A Box-Wilson Central Composite Design normally called 'a focal composite configuration,' contains an imbedded factorial or fragmentary factorial outline with focus focuses that is enlarged with a gathering of `star focuses' that permit estimation of arch. In the event that the separation from the focal point of the outline space to a factorial point is ±1 unit for each factor, the separation from the focal point of the plan space to a star point is ±α with | α | > 1. The exact estimation of α relies upon specific properties wanted for the plan and on the quantity of components included. Also, the quantity of focus point runs the plan is to contain additionally relies upon specific properties required for the plan.

3.17 RESIDUAL STRESSES IN WELDING

Residual stresses can be defined as that stress that is locked inside the engineering parts even when there is no outside load and these grow fundamentally due to a non-uniform volumetric change in metallic segment independent of manufacturing procedures, for example, machining, heat treatment, mechanical distortion, casting, welding, coating and so on. In any case, most extreme estimation of residual stress doesn't surpass the maximum value of the metal elastic limit since stresses higher than elastic limit prompts plastic deformation and residual stresses are accommodated as distortions. Residual stresses can be tensile or compressive depending up on the area and kind of non-uniform volumetric change occurring because of differential heating and cooling like in welding and heat treatment or confined stresses like in contour, machining, rolling and shotpeening and so forth.

Residual stress in welded joints essentially develop because of differential weld heat cycle (heating, peak temperature and cooling at any minute amid welding) experienced by the weld metal and area closed to fusion limit i.e. heat influenced zone. Type and magnitude of the residual stress change persistently amid various phases of welding i.e. heating and cooling. Amid heating principally compressive residual stress is created in the region of base metal which is being heated for softening because of heat

extension and the same (thermal expansion) is limited by the low temperature encompassing base metal. Subsequent to achieving a peak value compressive residual stress continuously diminishes attributable to softening of metal being heated. During cooling as metal starts to shrink, tensile residual stresses develop (only if shrinkage is not allowed either due to metallic continuity or constraint from job clamping) and their magnitude keeps on increasing until room temperature is attained. In general, the value of residual stresses directly proportional to degree of constraint and elastic limit of melting material.

3.17.1 EFFECTS OF RESIDUAL STRESSES

The residual stresses affects the soundness, dimensional stability and mechanical performance of the weld joints irrespective of tensile or compressive nature. Since extent of residual stress rises gradually to peak value until the point when weld joint is chilled off to the room temperature subsequently for the most part the impacts of residual stresses are watched either close to the last phase of welding or after some time of welding as cracks (hot cracking, lamellar tearing, cold cracking), distortion and reduction in mechanical performance of the weld joint and mechanical execution of the weld joint As residual streses are both positive or negative in nature, its presence in the weld joints can increase or decrease failures due to external loading. Residual stress of the same nature as that of external load enhances the failure tendency while that of opposite nature reduces the same. Since most failures of mechanical part happens under tensile load by break nucleation and their propagation under tensile conditions therefore presence of tensile residual stresses in combination with external tensile loading adversely affect the performance in respect of tensile load carrying capacity while compressive residual stresses under similar loading conditions defines the net stresses and so it reduces the failure tendency.

3.17.2 Determination of Residual Stress

Residual stresses are the stresses which exist within a component or structure in the absence of any external forces, or it can be defined as the stresses which remains inside a body which is either stationary or at equilibrium with its surroundings. These stresses can be beneficial or detrimental depending upon its nature, to the performance and the service life period of the component. However, beneficial residual stresses can

also be induced intentionally to nullify the detrimental effect of already existing stresses. It is really a very difficult and complex task to predict the residual stresses than the load stresses usually they superimpose on them, Due to this reason, it is very essential to have some reliable, accurate, precise and faster methods for the measurement of residual stresses.

Presently, there are a large number of methods available that can be used for the measurement of residual stress, these are destructive and non-destructive methods. Destructive methods are hole drilling method, crack compliance method etc. while non-destructive methods are x-ray diffraction, neutron diffraction etc. can be used without causing any significant destruction to the component; some have excellent spatial resolution, whereas others are restricted to near surface stresses or to the certain specific classes of material. In the case of destructive methods, a distinction should be made between partial and total destruction. Partial destruction involves generating small holes or grooving rings throughout the surface of the testing object or component, which allows the part to be used further.

3.17.2.1 X-RAY DIFFRACTION

Using the portable equipment μ-X360n, the residual stresses are measured up-to the depths of 30μm by measuring the inter-atomic spacing of material.

X-rays have wavelength of same order as the inter-planar distances in materials. When X-rays strike the surface of materials it gets scattered to form constructive to destructive interference of a diffracted beam. The equipment also measures the angle of maximum diffraction interference. The angles measured from interferences will be used to measure inter planar distances (d_0). The presence of residual stress in sample changes the d spacing which can be measured with the help of bragg's law. The difference of d-spacing according to bragg's law is directly proportional to strain which can be used to calculate residual stress.

3.17.3 Cosα Method

The standard $Sin^2\Psi$ approach with a point detector (diffractometer) requires a series of measurements at different orientations of the sample with respect to diffractometer to obtain the projection of the strain tensor along the several different orientations of the scattering vector, and these orientations are chosen so as to simplify the subsequent analysis (Ling and Lee 2015).

Since for a defined sample orientation in laboratory coordinates every point in the Debye ring comes from a different orientation of the scattering vector, when using a 2D detector the whole

Debye ring can be used and a set of scattering vector orientations are simultaneously probed in a single measurement. Among the analysis methods that can be used to extract the stress state from such information with a single measurement, the "cosα" method was first proposed by Taira (Taira et al, 1978).

Nowadays, use of portable residuals stress analyzers have seen increased due to the ease of its use. The cosα method has emerge as a faster and easier method of measuring residual stresses experimentally by using portable devices due to its ability to measure an entire Debye ring at once from the two dimensional detector, thus not requiring multiple sample tilts as in case of $Sin^2\Psi$ method (Kobayashi et al. 2017).

3.17.4 Portable X-Ray Device to Measure Residual Stress by using Cosα method

A portable X-ray device (μ-X360 residual stress analyzer from Pulstec Industrial Co.Ltd.) mounted on a robust table, is used to measure the residual stresses after springback in TWBs specimens. Various points are marked across the width of the specimen after bending along the bend axis on thicker and thinner sheets both on compression and tension side. Detector gun of the stress analyzer is inclined at an angle of 35° for the IF Steel (Ferrite).

Specimen is placed on the adjustable table exposing the surface to be assessed for the residual stress establishing a red spot of laser (approximately 2mm) on the mark where the X-ray beam will incident. The specifications of X-ray machine are given in table 3.4

Table 3.4: Specifications of the X-ray machine (μ-X360)

X-ray Tube Voltage, Current	30 KV, 1.0 Ma
Target Material	Chromium (Cr)
Beam Wavelength (Energy)	λ= 2.29 Å (E = 5.4 KeV)
Collimator and Beam Spot Size	1 mm and 2 mm diameter
Sample to Detector Distance Approx.	35-40 mm
Typical Data Acquisition + Readout Time	90 seconds

CHAPTER 4

EXPERIMENTATION

The purpose of the experimentation is to see the effects of input parameters on the bead geometry of SAW and to generate mathematical models to describe the relationship among various parameters. For achieving above objectives, following are the steps were carried out:

1. Identification of essential process control factors
2. Deciding the working scope of the procedure control factors, viz. Circular segment Voltage (V), Current (A), Travel Speed (S) and Nozzle-to-plate-separate (N)
3. Developing the design matrix
4. Conducting the examinations according to the design matrix
5. Recording the reactions viz. Bead height (H), bead width (W) and penetration of bead (P)
6. Developing the numerical models
7. Checking the adequacy of the models
8. Finding the significance of coefficient
9. Developing the final proposed models
10. Plotting of diagrams and drawing conclusion
11. Discussion of the outcomes

4.1   Identification of numerous process control factors

Based on the impact on weld bead geometry, simplicity of control and capacity of being maintained at desire level, three independent controllable process parameters were recognized to be specific, the arc voltage (V); percentage of iron powder and the travel speed. The weld bead geometry parameters decided for this examination were reinforcement height (H), bead width (W) and penetration (P).

4.2 Deciding the range of the process factors

Preliminary runs were led by differing one of the process parameters at once while keeping whatever remains of them at constant value. The working range was fixed by inspecting the bead for a smooth appearance and the nonappearance of obvious deformities.

The upper and lower limits were coded as +2 and −2, individually. The coded esteems for middle of the road esteems can be computed from the relationship, Where, Xi is the required coded estimation of a variable X, when X is any estimation of the variable from Xmin to Xmax; Xmax and Xmin are the most extreme and least levels of the factors. They chose procedure parameters and their upper and lower restrains together with documentations and units are given in Table 4.1.

Table 4.1: Process control parameters and their breaking points

S.NO.	Parameters	Units	Notations	-2	-1	0	+1	+2
1.	Travel speed	Cm/sec	S	38	40	42	44	46
2.	Arc voltage	Volt	V	29	31	33	35	37
3.	% iron powder	%	%	0	5	10	15	20

4.3 Developing the design framework

A completely rotatable 3 factor 5 level composite design matrix was utilized for the experiment. A completely rotatable central composite design matrix covers more noteworthy design space than the factorial design matrix lattice, consequently bringing about more prominent exactness of the established relationship [43]. Table 4.2 demonstrates the 20 sets of coded conditions used to frame the outline lattice.

Table 4.2: Design matrix

Weld no.	Trial no.	Coded value of velocity	Coded value of voltage	Coded value % Fe	Actual value of velocity(cm.)	Actual value of voltage (volt)	Actual value of %fe
15	1	0	0	0	42	33	10
6	2	1	-1	1	44	31	15
12	3	0	2	0	42	37	10
4	4	1	1	-1	44	35	5
18	5	0	0	0	42	33	10
7	6	-1	1	1	40	35	15
14	7	0	0	2	42	33	20
11	8	0	-2	0	42	29	10
5	9	-1	-1	1	40	31	15
16	10	0	0	0	42	33	10
8	11	1	1	1	44	35	15
20	12	0	0	0	42	33	10
17	13	0	0	0	42	33	10
3	14	-1	1	-1	40	35	5
2	15	1	-1	-1	44	31	5
1	16	-1	-1	-1	40	31	5
10	17	2	0	0	46	37	10
19	18	0	0	0	42	33	10
13	19	0	0	-2	42	33	0
9	20	-2	0	0	38	33	10

4.4 Perform the experiments as per the design matrix

The welding experiment was conducted at the welding laboratory of NSIT Delhi with the following experimental set-up:

Figure 4.1: The SAW machine used for the experiment

4.5 Machine model and material used:

CPRA800, Manufactured by- ESAB INDIA LIMITED, P-18 Taratala road Calcutta-88. The welding wire of 3.2 mm diameter copper coated mild steel wire manufactured by ESAB INDIA LIMITED was used. AWS-A5.17 EL-8 is the specification of welding wire used. The chemical composition of welding wire was:

Table 4.1: Chemical composition of work piece material

%C	%Si	%Mn
0.10	0.02	0.45

For carrying out experimental work, the work specimen prepared from 12 Mm thick AISI1012 Mild steel plate. 260*60*12 mm. Composition of the material as follows:

Table 4.2 Chemical composition of filler material

%C	%Mn	%Si	%Ni	%S	%Cr
0.10-0.102	0.466	0.179	0.022	0.0705	0.036

4.6 Type of joint:

The welding is done on the Bead on plate types.

4.7 Flux:

The flux was manufactured by ESAB INDIA LTD. The flux specified by following way: Auto melt Gr. 2, Coding-AWS/SFA 5.17, F7AZ-EL8; F7PZ-EL8

Table 4.6 The chemical composition of flux

C	Mn	Sn
0.08%	1.00%	0.25%

Figure 4.2: welded sample

4.9 Recording of results

After done the welding process, put the plates in the natural environment and then remove the slag layer by using hammer, sometimes it will automatically taken out from the bead. The welded plate cut into 3 parts in transverse direction.

Now perform dry and wet polishing of a given mild steel specimen and then etching the weld bead by acid. First of all it is necessary to obtain a reasonable surface with a file or grinder. Now dry polishing are carried out by emery papers of grades 100, 200, 320, 600 and 1000 and the grade size when a bright surface is obtain then we go for wet polishing by using alumina powder and water mixture. After wet polishing etching will be perform with the help of the solution of 2% nitric acid and 98% water. All the sequence-wise operation are shown in following figures.

Figure 4.3 : power hacksaw	Figure 4.4 : specimen after cut by power hacksaw
Figure :4.5 Rough grinding	Figure : 4.6 Wet polishing
Figure :4.7 Weld bead after wet polishing	Figure: 4.8 weld bead after etching

Table 4.4 Recording of responses

Weld no.	Trial no.	Coded value of velocity	Coded value of voltage	Coded value % Fe	penetration (p)	Reinforcement (H)	Bead width (W)	Residual stress
15	1	0	0	0	5.76	3.25	11.6	146
6	2	0	0	0	5.76	3.25	11.76	158
12	3	-1	-1	-1	5.55	3.54	10.9	114
4	4	0	0	2	7.08	3.45	12.32	220
18	5	1	1	1	6.83	3.15	12.78	190
7	6	1	-1	1	5.32	3.13	10.56	119
14	7	1	1	-1	5.26	2.6	12.14	131
11	8	-1	1	1	7.88	3.61	13.64	211
5	9	0	2	0	7.54	2.2	14.14	207
16	10	-1	-1	1	6.27	3.17	11.51	158
8	11	1	-1	-1	3.45	3.12	10.05	74
20	12	-1	1	-1	6.31	3.06	13.03	183
17	13	0	0	0	5.52	3.05	11.6	146
3	14	0	0	0	5.76	3.05	11.76	158
2	15	2	0	0	4.88	2.88	10.86	108
1	16	-2	0	0	6.91	4.56	12.54	171
10	17	0	0	0	5.52	3.25	11.6	158
19	18	0	-2	0	4.53	2.96	9.86	86
13	19	0	0	0	5.62	3.25	11.66	146
9	20	0	0	-2	3.92	2.95	10.75	131

Chapter 5

STATISTICAL ANALYSIS

Mathematical models can be proposed as the basis for a control system for the SAW process to predict particular weld bead geometry and to establish the interrelationship between weld process parameters to weld bead geometry. These mathematical models can be fed into computer to predict the weld bead geometry for a particular combination of input parameters. The experimental data were used to develop nonlinear models, and analysis of the models was carried out through ANOVA and surface plots. Design expert 11.0.6 was used for this purpose.

5.1.1 Developments of mathematical models:

The response function representing any of the weld-bead dimensions can be expressed as:

Y = f (V, S, %Fe)

Y = Weld bead response;

V = Arc voltage;

%Fe = %age of iron powder;

S = travel speed.

5.1.2 DESIGN EXPERT VERSION 11.0.6 SOFTWARE

Design expert software is very useful in making leap forward changes to an item or a procedure. We can screen for essential elements, as well as find perfect process settings for top execution and find ideal item details. We can effortlessly see response surfaces from all points with rotatable 3D plots. We can Set flags and investigate forms on intuitive 2D diagrams; and can utilize the numerical enhancement capacity to discover most extreme functions for many reactions simultaneously.

5.2 Checking adequacy of the model

The analysis of variance (ANOVA) technique was used to check the adequacy of the developed models. As per this technique:

1. The F-ratio of the developed model is calculated and is compared with the standard tabulated value of F-ratio for a specific level of confidence

2. If calculated value of F-ratio does not exceed the tabulated value, then with the corresponding confidence probability the model may be considered adequate. For our analysis, we have taken a confidence interval of 95%.

5.3 Response: Bead Height

The fit summary for reinforcement height is given in table 5.1. The quadratic model is suggested for the analysis of bead height.

Table 5.1 fit summary for reinforcement height

Source	Sum of square	Df	Mean square	F-value	p-value	
Mean vs Total	213.86	1	213.86			
Linear vs Mean	0.5051	3	0.1684	0.4708	0.7069	
2FI vs Linear	0.3110	3	0.1037	0.2490	0.8606	
Quadratic vs 2FI	**4.81**	**3**	**1.60**	**26.74**	**< 0.0001**	**Suggested**
Cubic vs Quadratic	0.2985	4	0.0746	1.49	0.3159	
Residual	0.3012	6	0.0502			
Total	220.09	20	11.00			

Table 5.2 ANOVA for reinforcement height

S.NO.	Source	Sum of squares	df	Mean square	F-value	p-value	
	Model	1.64	9	0.1828	10.78	0.0014	Significant
1.	A-	0.2381	1	0.2381	14.04	0.0045	

	velocity						
2.	B-voltag0e	0.2652	1	0.2652	15.64	0.0042	
3.	C-iron powder	0.0181	1	0.0181	11.16	0.0102	
4.	AB	0.0264	1	0.0264	1.56	0.2470	
5.	AC	0.0181	1	0.0181	1.06	0.3323	
6.	BC	0.2665	1	0.2665	15.72	0.0042	
7.	A^2	0.0805	1	0.0805	4.75	0.0609	
8.	B^2	0.5460	1	0.5460	32.21	0.0005	
9.	C^2	0.0004	1	0.0004	0.0246	0.8793	
10.	Residual	0.1356	8	0.0170			
11.	Lack of fit	0.0823	3	0.0274	2.57	0.1672	Not significant
12.	Pure error	0.0533	5	0.0107			
13.	Cor Total	1.78	17				

The model F value of 10.78 implies that the model is significant. There is only a 0.14% chance that a "Model F- value" this large could occur due to noise. Values of "Prob>F" less than 0.0500 indicates that model terms are significant. In this case A, B, C, BC, and B^2 are significant model terms. Values greater than 0.1000 indicate the model terms are not significant. The "Lack of Fit F-value" of 2.57 implies that the Lack of fit F-value is not significant relative to the pure error. There is 16.72% chance that a "Lack of fit F-value" this large could occur due to noise. Non- significant Lack of fit is good- we want the model to fit. The " pred R-Squared" is 0.2173 which is in reasonable agreement with the " Adj R-   sqared" which is 0.8381. "Adeq Precision" measures the signal to noise ratio. A ratio greater

than 4 is desirable. The Adeq Precision obtained for our model is 12.5191, which indicates an adequate signal. This model can be used to explore the design space.

Table 5.3 ANOVA reinforcement height after forward elimination

S.NO.	Source	Sum of squares	Df	Mean square	F-value	p-value	
	Model	1.60	6	0.2666	16.25	<0.0001	Significant
1.	A-velocity	0.2380	1	0.2380	14.50	0.0029	
2.	B-voltag0e	0.2652	1	0.2652	16.16	0.0020	
3.	C-iron powder	0.1892	1	0.1892	11.53	0.0060	
4.	BC	0.2665	1	0.2665	16.23	0.0020	
5.	A^2	0.0827	1	0.0827	5.04	0.0463	
6.	B^2	0.5905	1	0.5905	35.98	<0.0001	
7.	Residual	0.1806	11	0.0164			
8.	Lack of fit	0.1272	6	0.0212	1.99	0.2340	Not significant
9.	Pure error	0.0533	5	0.0107			

10.	Cor Total	1.78	17				

It has been observed from table 5.3, that F-value increases from 10.78 to 16.25 and p-value decreases from 1.4% to less than 1% after forward elimination. The adjusted R^2 value is 0.8433 , predicted R^2 value is 0.4749 and Adeq precision is 15.3328 after the forward elimination process.

5.4 <u>Response : Bead Width</u>

Table 5.4 fit summary for bead width

Source	Sum of square	Df	Mean square	F-value	p-value	
Mean vs Total	2762.66	1	2762.66			
Linear vs Mean	23.22	3	7.74	318.33	< 0.0001	
2FI vs Linear	0.0030	3	0.0010	0.0341	0.9911	
Quadratic vs 2FI	**0.2687**	**3**	**0.0896**	**7.64**	**0.0061**	**Suggested**
Cubic vs Quadratic	0.0414	4	0.0104	0.8195	0.5571	
Residual	0.0758	6	0.0126			
Total	2786.27	20	139.31			

Table 5.5 ANOVA for bead width

S.NO.	Source	Sum of squares	Df	Mean square	F-value	p-value	
	Model	23.49	9	2.61	222.60	< 0.0001	Significant
1.	A-velocity	2.98	1	2.98	254.48	< 0.0001	
2.	B-voltage	18.34	1	18.34	1563.93	< 0.0001	
3.	C-iron powder	1.90	1	1.90	161.81	< 0.0001	
4.	AB	0.0003	1	0.0003	0.0266	0.8736	
5.	AC	0.0006	1	0.0006	0.0522	0.8238	
6.	BC	0.0021	1	0.0021	0.1801	0.6802	
7.	A^2	0.0085	1	0.0085	0.7266	0.4139	
8.	B^2	0.2194	1	0.2194	18.71	0.0015	
9.	C^2	0.0131	1	0.0131	1.12	0.3151	
10.	Residual	0.1173	10	0.0117			
11.	Lack of fit	0.0865	5	0.0173	2.82	0.1402	not significant
12.	Pure error	0.0307	5	0.0061			
13.	Cor Total	23.61	19				

The model F-value of 222.60 implies the model is significant. There is only a 0.01% chance that a "Model F-value" this large could occur due to noise. Values of "Prob > F" less than 0.0500 indicates model terms are significant. In this case B, BC and B^2 are significant model terms. Values greater than 0.1000 indicates the model terms are not significant. The "lack of Fit F-value" of 2.82 implies the lack of fit is not significant relative to the pure error. There is a 14.02% chance that a "Lack of fit F-value" this large could occur due to noise. Non-significant lack of fit is good- we want the model to fit. The "pred R-squared" is 0.9685 which is in reasonable agreement with the "Adj R- squared" of 0.9906. "adeq Precison" measures the signal

to noise ratio. A ratio greater than 4 is desirable. . The "Adeq Precision" obtained for our model is 86.30 which indicate an adequate signal. This model can be used to navigate the design space.

Table 5.6 ANOVA for bead width after forward elimination

S.NO.	Source	Sum of squares	Df	Mean square	F-value	p-value	
	Model	23.46	4	5.87	595.57	< 0.0001	Significant
1.	A-velocity	2.98	1	2.98	303.00	< 0.0001	
2.	B-voltage	18.34	1	18.34	1862.12	< 0.0001	
3.	C-iron powder	1.90	1	1.90	192.66	< 0.0001	
8.	B^2	0.2413	1	0.2413	24.50	0.0002	
10.	Residual	0.1477	15	0.0098			
11.	Lack of fit	0.1170	10	0.0117	1.90	0.2474	not significant
12.	Pure error	0.0307	5	0.0061			
13.	Cor Total	23.61	19				

By comparing table 5.3 and table 5.4, we conclude that our F-value increases from 222.60 to 595.57 and p-value is less than 1%. The "pred R-squared" is 0.9868 which is in reasonable agreement with the "Adj R- squared" of 0.9921. Adeq precision is 86.30 after the forward elimination process.

5.5 Response: Bead Penetration

The fit summary for bead penetration is shown in table 5.7. Based on the suggested model, quadratic model is selected for analysis of bead penetration.

Table 5.7 fit summary for bead penetration

Source	Sum of square	Df	Mean square	F-value	p-value	
Mean vs Total	668.98	1	668.98			
Linear vs Mean	22.95	3	7.65	110.38	< 0.0001	
2FI vs Linear	0.3159	3	0.1053	1.73	0.2107	
Quadratic vs 2FI	**0.4208**	**3**	**0.1403**	**3.77**	**0.0480**	**Suggested**
Cubic vs Quadratic	0.2681	4	0.0670	3.87	0.0688	
Residual	0.1038	6	0.0173			
Total	693.03	20	34.65			

Table 5.8 ANOVA for Bead penetration

S.NO.	Source	Sum of squares	df	Mean square	F-value	p-value	
	Model	23.68	9	2.63	70.75	< 0.0001	Significant
1.	A-velocity	5.30	1	5.30	142.53	< 0.0001	
2.	B-voltage	8.57	1	8.57	230.41	< 0.0001	
3.	C-iron powder	9.08	1	9.08	243.98	< 0.0001	
4.	AB	0.1128	1	0.1128	3.03	0.1122	
5.	AC	0.1653	1	0.1653	4.44	0.0612	
6.	BC	0.0378	1	0.0378	1.02	0.3371	
7.	A^2	0.1146	1	0.1146	3.08	0.1098	
8.	B^2	0.2642	1	0.2642	7.10	0.0237	
9.	C^2	0.0246	1	0.0246	0.6601	0.4354	
10.	Residual	0.3720	10	0.0372			

11.	Lack of fit	0.3012	5	0.0602	4.26	0.0689	not significant
12.	Pure error	0.0707	5	0.0141			
13.	Cor Total	24.06	19				

The model F-value of 70.75 implies the model is significant. There is only a 0.01% chance that a "Model F-value" this large could occur due to noise. Values of "Prob >F" less than 0.0500 indicate the model terms are significant. In this case A, B, C, and B^2 are significant model terms. Values greater than 0.100 indicate the model terms are not significant. The "lack of fit F-value" of 4.26 implies that the lack of fit is not significant relative to the pure error. There is a 6.89% chance that a "Lack of fit F-value" this large could occur due to noise. Non-significant lack of fit is good- we want the model to fit. The "pred R squared" is 0.9017 is in reasonable agreement with the "Ädj R-squared" of 0.9706. "adeq Precision" measures the signal to noise ratio. A ratio greater than 4 is desirable. The Adeq Precision obtained for our model is 30.22 indicates an adequate signal.

Table 5.9 ANOVA for penetration after forward elimination

S.NO.	Source	Sum of squares	df	Mean square	F-value	p-value	
	Model	23.36	5	4.67	94.51	< 0.0001	Significant
1.	A-velocity	5.30	1	5.30	107.22	< 0.0001	
2.	B-voltage	8.57	1	8.57	173.33	< 0.0001	
3.	C-iron powder	9.08	1	9.08	183.55	< 0.0001	
5.	AC	0.1653	1	0.1653	3.34	0.0889	
7.	B^2	0.2512	1	0.2512	5.08	0.0407	
10.	Residual	0.6922	14	0.0494			

11.	Lack of fit	0.6215	9	0.0691	4.88	0.0478	Not significant
12.	Pure error	0.0707	5	0.0141			
13.	Cor Total	24.06	19				

After comparing table 5.8 and table 5.9, we can conclude that F value of our model increases From 70.75 to 94.950 The adjusted R^2 value is 0.9609, predicted R^2 value is 0.9331 and the Adeq precision is 33.83, after the forward elimination process.

5.5 Response: Residual stress

The fit summary for bead penetration is shown in table 5.10. Based on the suggested model, quadratic model is selected for analysis of bead penetration.

Table 5.10 fit summary for Residual stress

Source	Sum of square	Df	Mean square	F-value	p-value	
Mean vs Total	4.545E+05	1	4.545E+05			
Linear vs Mean	27791.50	3	9263.83	70.04	< 0.0001	
2FI vs Linear	133.00	3	44.33	0.2906	0.8314	
Quadratic vs 2FI	**1457.64**	**3**	**485.88**	**9.24**	**0.0031**	**Suggested**
Cubic vs Quadratic	159.00	4	39.75	0.6505	0.6473	Aliased
Residual	366.61	6	61.10			
Total	4.844E+05	20	24220.95			

Table 5.11 ANOVA for Residual stress

S.NO.	Source	Sum of squares	df	Mean square	F-value	p-value	
	Model	29382.14	9	3264.68	62.11	< 0.0001	Significant
1.	A-velocity	4830.25	1	4830.25	91.90	< 0.0001	
2.	B-voltage	15129.00	1	15129.00	287.83	< 0.0001	

41

S.NO.	Source	Sum of	df	Mean	F-	p-value	
3.	C-iron powder	7832.25	1	7832.25	149.01	< 0.0001	
4.	AB	4.50	1	4.50	0.0856	0.7758	
5.	AC	128.00	1	128.00	2.44	0.1497	
6.	BC	0.5000	1	0.5000	0.0095	0.9242	
7.	A^2	336.64	1	336.64	6.40	0.0298	
8.	B^2	91.64	1	91.64	1.74	0.2161	
9.	C^2	717.21	1	717.21	13.65	0.0041	
10.	Residual	525.61	10	52.56			
11.	Lack of fit	309.61	5	61.92	1.43	0.3512	not significant
12.	Pure error	216.00	5	43.20			
13.	Cor Total	29907.75	19				

The model F-value of 62.11 implies the model is significant. There is only a 0.01% chance that a "Model F-value" this large could occur due to noise. Values of "Prob >F" less than 0.0500 indicate the model terms are significant. In this case A, B, C, A^2, and C^2 are significant model terms. Values greater than 0.100 indicate the model terms are not significant. The "lack of fit F-value" of 1.43 implies that the lack of fit is not significant relative to the pure error. There is a 35.12% chance that a "Lack of fit F-value" this large could occur due to noise. Non-significant lack of fit is good- we want the model to fit. The "pred R squared" is 0.9112 is in reasonable agreement with the "Ädj R-squared" of 0.9666. "adeq Precision" measures the signal to noise ratio. A ratio greater than 4 is desirable. The Adeq Precision obtained for our model is 27.5520 indicates an adequate signal. This model can be used to navigate the design space.

Table 5.13 ANOVA for residual stress after forward elimination

S.NO.	Source	Sum of	df	Mean	F-	p-value	

		squares		square	value		
	Model	29157.50	5	5831.50	108.82	< 0.0001	significant
1.	A-velocity	4830.25	1	4830.25	90.13	< 0.0001	
2.	B-voltage	15129.00	1	15129.00	282.31	< 0.0001	
3.	C-iron powder	7832.25	1	7832.25	146.15	< 0.0001	
5.	A^2	278.35	1	278.35	5.19	0.0389	
7.	B^2	871.29	1	871.29	16.26	0.0012	
10.	Residual	750.25	14	53.59			
11.	Lack of fit	534.25	9	59.36	1.37	0.3800	not significant
12.	Pure error	216.00	5	43.20			
13.	Cor Total	29907.75	19				

After comparing table 5.8 and table 5.9, we can conclude that F value of our model increases From 62.110 to 108.82. The adjusted R^2 value is 0.9660 predicted R^2 value is 0.9401 and the Adeq precision is 35.0410, after the forward elimination process.

5.6 Design matrix and nonlinear equation

The value of coefficient of response surface was calculated using regression analysis. The calculations were carried out using design expert 11.0.6 and values listed in table 5.10.

Table 5.14 estimated value of the coefficient of the model

S. NO.	Coefficient	Reinforcement height (h)	Bead Width (w)	Penetration (p)	Residual stress
1	Intercept	+3.18	+11.93365	+5.82485	+150.93

S. NO.	Coefficient				
2	A-velocity	-0.1725	-0.478485	+0.094779	-17.38
3	B-voltage	-0.1288	+0.502464	+0.077279	+30.75
4	C-iron powder	+0.1087	+0.284015	+0.512500	+22.13
5	AB	-0.0575	+1.15447	+0.705000	+0.7500
6	BC	+0.0475	-0.604015	-0.225000	+4.00
7	AC	+0.1825	-0.048029	+0.122500	-0.2500
8	A^2	+0.1358	-0.181925	+0.065956	-3.66
9	B^2	-0.1508	-0.089425	-0.047794	-1.91
10	C^2	+0.0042	-0.280675	-0.295074	+5.34

Table 5.16 estimated value of the coefficient of the model after forward elimination

S. NO.	Coefficient	Reinforcement height (h)	Width (w)	Penetration (p)	Residual stress
1	Intercept	+3.19	+11.68	+5.70662	+148.75000
2	A-velocity	-0.1725	-0.4319	-0.575625	-17.37500
3	B-voltage	-0.1288	+1.07	+0.731875	+30.75000
4	C-iron powder	+0.1087	+0.3444	+0.753125	+22.12500
5	AB	-	-	-	-
6	BC	+0.1825	-	-	-
7	AC	-	-	+0.1438	-
8	A^2	+0.1369	-	-	-3.25
9	B^2	-0.1519	+0.0942	+0.0961	-
10	C^2	-	-	-	-

CHAPTER 6

RESULT ANALYSIS AND DISCUSSION
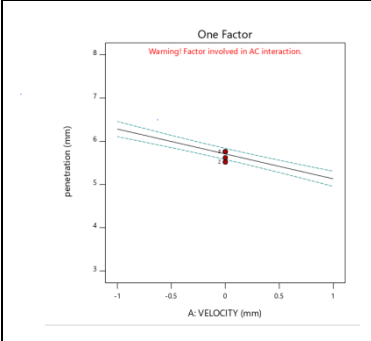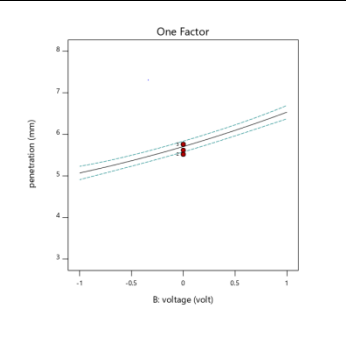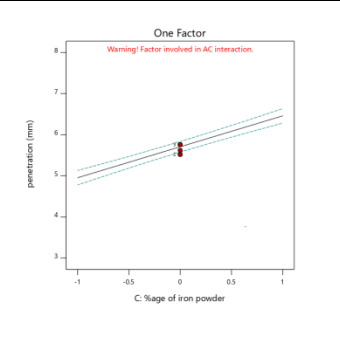
The mathematical models developed above can be employed to predict the geometry of weld bead and shape relationships for the range of parameters used in the investigation by substituting their respective values in coded form. Based on these models, the main and the interaction effects of the process parameters on the bead geometry were computed and plotted as depicted in Figs. The results show the general trends between cause and effect.

6.1 Interaction effects of process variables on the bead parameters:

6.1.1 Direct Effect of process parameters on penetration

Direct Effect of input variables is shown in the table 6.1. As shown in fig(b) and fig(c), penetration increases continuesly with arc voltage and % of iron powder, because by adding iron powder thermal conductivity of weld zone is enhaces. As shown in fig(a), velocity having opposite effect on other two process parameters, this is happens because of increase in velocity there are less time given for heat transfer.
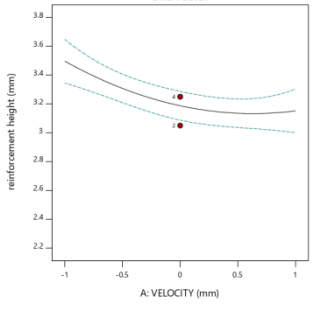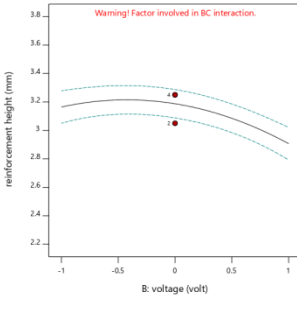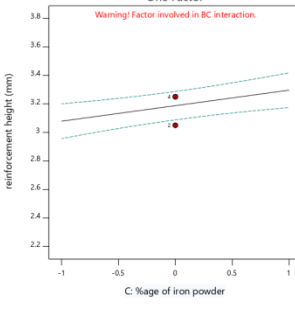
Table 6.1 Direct Effect of process parameters on penetration

| Figure (a) | Figure (b) | Figure (c) |

6.1.2 Direct Effect of process parameters on reinforcement height

Direct Effect of input variables is shown in the table 6.2. As shown in fig(a),by increasing the velocity, reinforcement height first decreases and then tends to a constant slope. Fig(b) shows the effect of voltage on reinforcement height, from here we conclude, the reinforcement height increases slightly and then decreases. By adding iron powder, reinforcement height increases continuesly
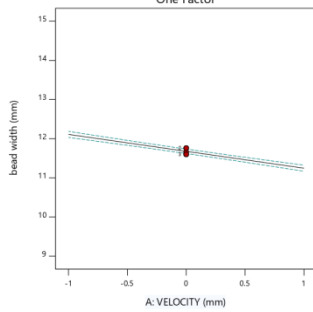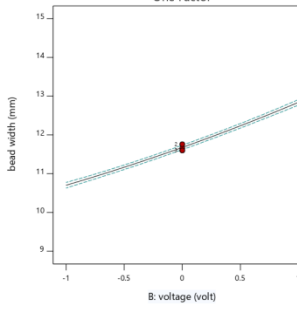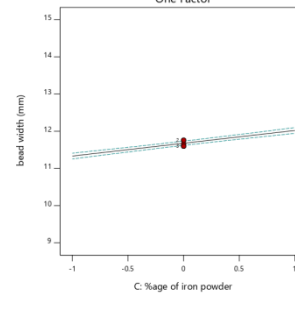
Table 6.2 Direct Effect of process parameters on reinforcement height

| Figure (a) | Figure (b) | Figure (c) |

6.1.3 Direct Effect of process parameters on bead width

Direct Effect of input variables is shown in the table 6.3. With the help of given table, we conclude that the effect of arc voltage is more on the bead width and very less affected by adding iron powder.

Table 6.3 Direct Effect of process parameters on bead width

| Figure (a) | Figure (b) | Figure (c) |

6.1.4 Direct Effect of process parameters on residual stress

Direct Effect of input variables is shown in the table 6.4, with the help of table 6.4, we conclude that, velocity having negative effect on residual stress whereas iron powder and arc voltage having positive effect on residual stress.

Table 6.4 Direct Effect of process parameters on residual stress

| Figure (a) | Figure (b) | Figure (c) |
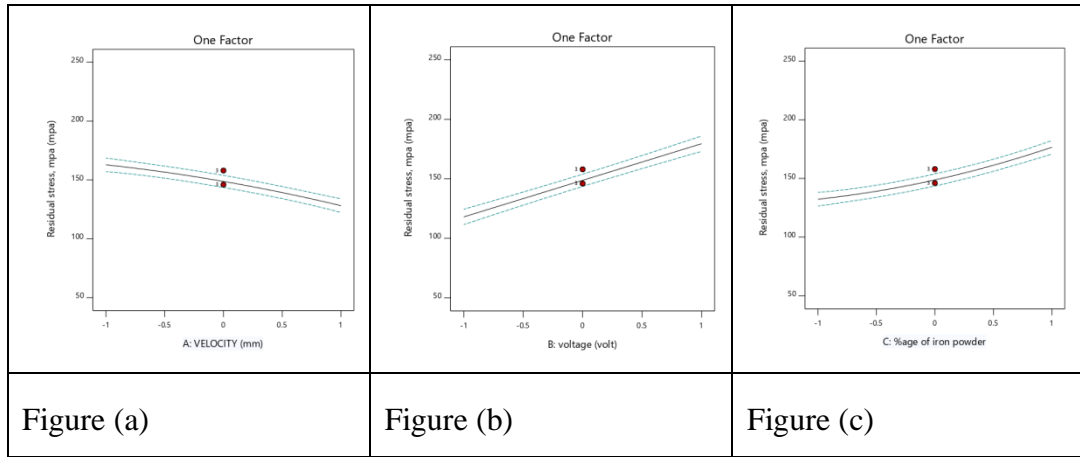
6.1.5 Effect of velocity and %age iron powder on penetration:

The interaction of voltage and velocity are shown in the table 6.5, from there we can conclude that, at lower level of velocity, by increasing the %age iron powder, the increase in penetration is more than the higher level of velocity. Depth of penetration decreases at both levels of iron powder by increasing the velocity, The maximum penetration get at lower level of velocity and higher level of iron powder, reason of this point is that there are good conduction of heat in that area and because of low speed the weld zone gets sufficient time for heat transfer.

Table 6.5 interaction of velocity and %age iron powder on penetration

| Figure(a): Interaction effect | Figure(b): Surface and contour plots |
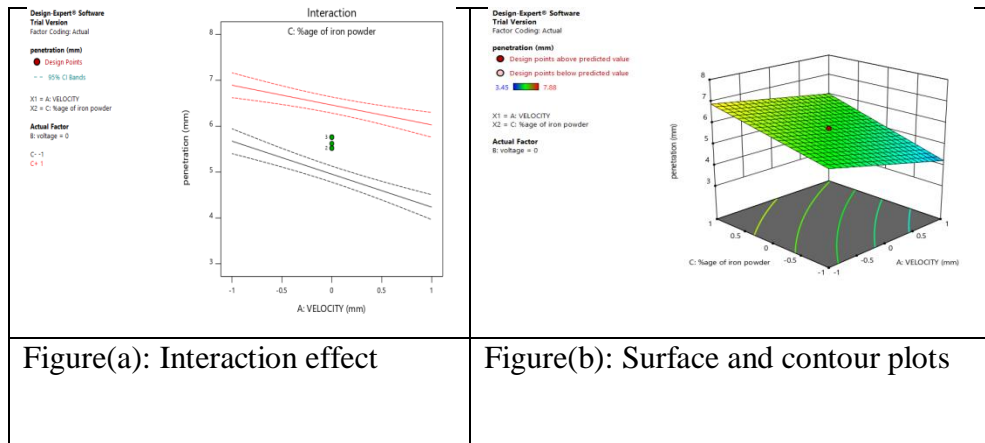
6.1.6   Effect of voltage and %iron powder on reinforcement height:

The interaction of voltage and iron powder are shown in the table 6.6, from there we can conclude that, at lower level of voltage there are negligible effect on reinforcement height by adding iron powder whereas at higher level of voltage there are increase in reinforcement height by adding iron powder. At higher level of iron powder, by increasing the voltage, reinforcement height decreases continuously. These interactions can be easily seen by rotating the three dimensional graph among voltage, iron powder and reinforcement height.

Table 6.6 interaction of voltage and %iron powder on reinforcement height

| Figure (a): Interaction effect | Figure (b): Surface and contour plots |
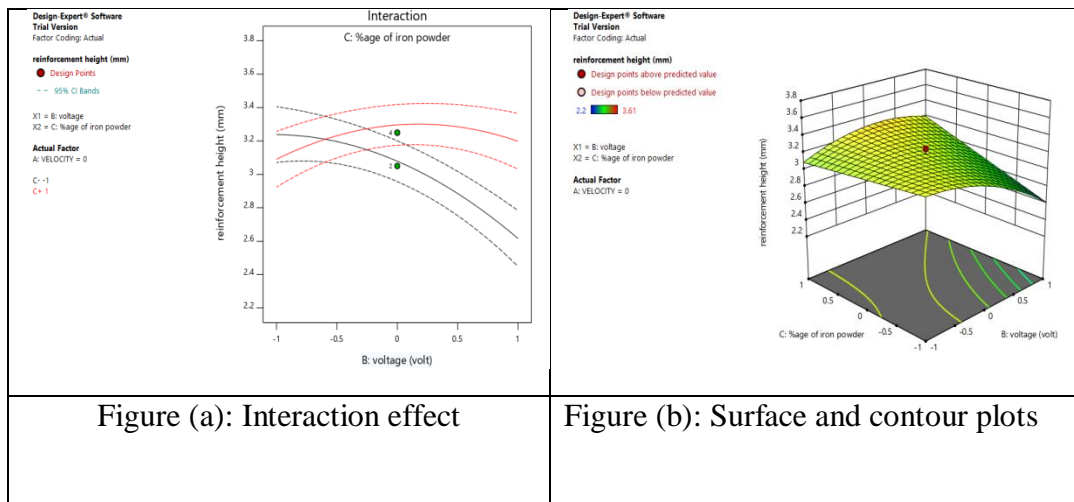
CHAPTER 7

MICROSTRUCTURE OF WELD BEAD

7.1 Introduction:

There are some changes in the weld metal after the welding process these changes can be understood by weld metallurgy. The requirement of study these changes arise because weld metallurgy directly affects the mechanical properties of weld joint. There are basically three main factors which affects the metallurgy which are how fast or slow heat is added, how fast or slow heat is removed and how much time be the joint will kept at elevated temperature. The main constituent of mild steel is iron and there are also 0.15-0.3% carbon, 0.4-0.7% manganese, 0.1-0.5% silicon and some other constituents.

7.2 Mild steel microstructure:
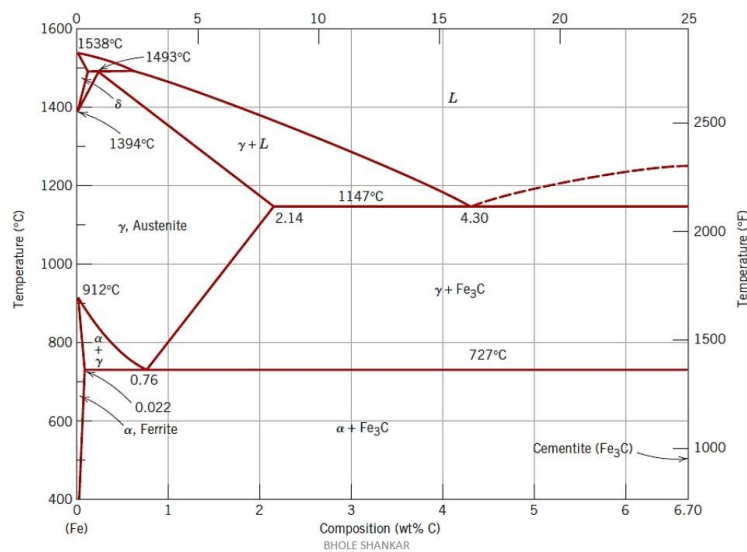
Figure 7.1 Fe-C phase diagram [22]

There are different allotropic forms of iron are shown in figure 3.12. Now we discussed these forms one by one:

- When solubility of carbon in iron is in between 0.08% to 0.02% at 723 degree centigrade, this is named as alpha ferrite. The crystal structure of ferrite is body centre cubic.

- When the solubility of carbon in iron is in the range of 0.8% to 2.08% and the temperature range is 723-1148 degree centigrade, the solution at that moment is known as austenite and it is having FCC structure. The carbon atoms are dissolved in iron interstitially.

- Cementite having 6.67% and 99.3% carbon and iron respectively such a large quantity of carbon makes it harder and stronger then ferrite and because of that reason cementite having less malleability. Crystal structure of Cementite is orthorhombic and having 12 and 4 atoms of Fe and C respectively.

- At 1493 degree centigrade maximum solubility of carbon is 0.09% in Fe at that time it is called as delta ferrite.

The steel classified according to carbon content as following,

OA - Hypo Eutectoid steel

AB - Hyper Eutectoid steel

BC - Hypo Eutectic steel

CD - Hyper Eutectic steel

As we seen the diagram mild steel having maximum carbon content of 0.3% so it is falls in the category of Hypo Eutectoid steel.
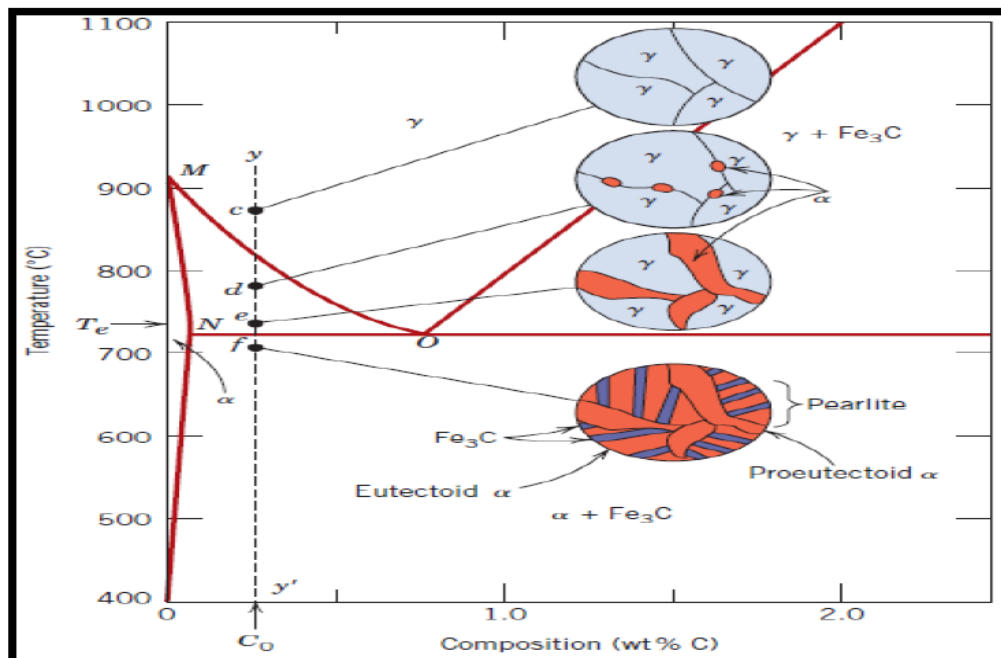
Fig 7.2 changing in microstructure during start of the process to reaching to the room temperature [23]

As we can see in the figure the 3.5 the point 'c', which entirely in gamma phase at just after the welding. From here slow cooling start and at the point 'd' two phases are exits there one is alpha and other is gamma phase whereas alpha phase are seen on the grain boundaries. The point 'e' is just above the eutectoid point the amount of alpha ferrite is increases on the grain boundaries. Now comes to point 'f' , here whole austenite is converted into the pearlite, this reaction also known as eutectoid reaction the alpha phase that is present at point 'e' is remains same.
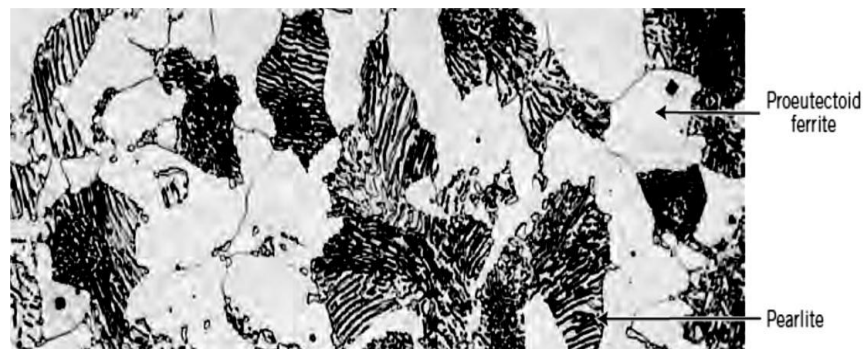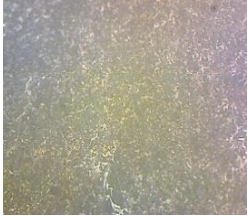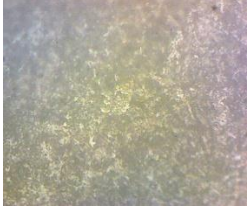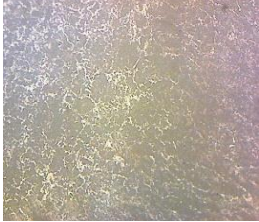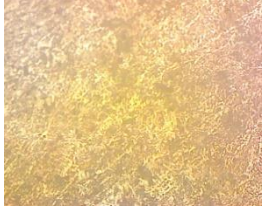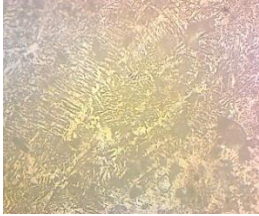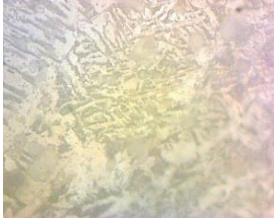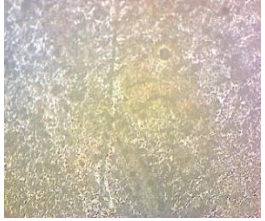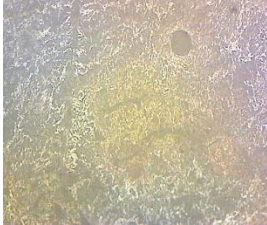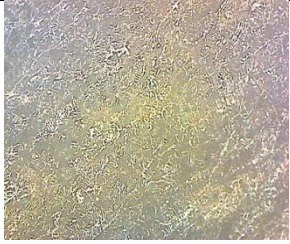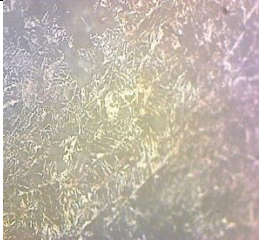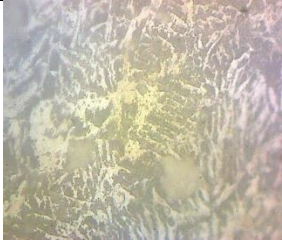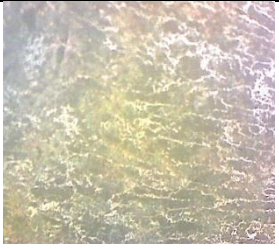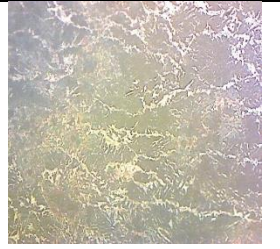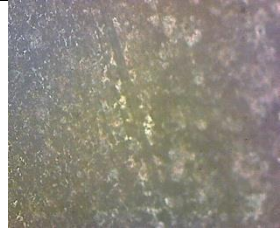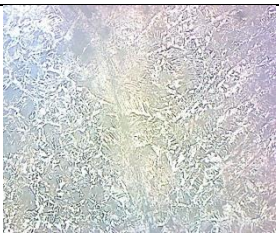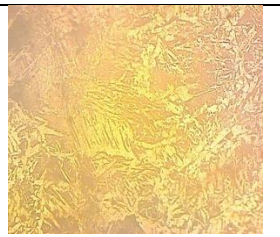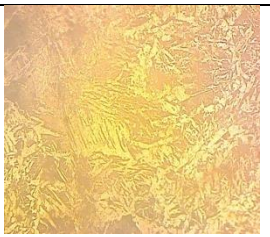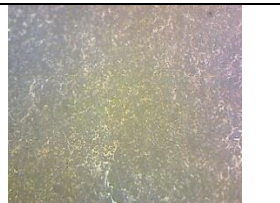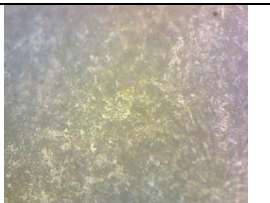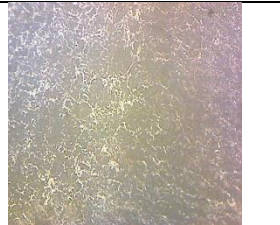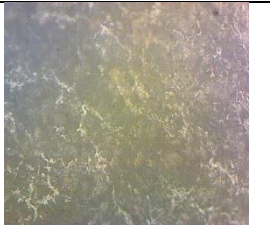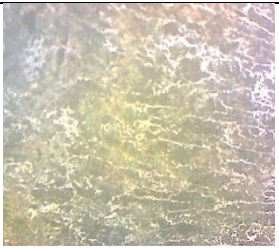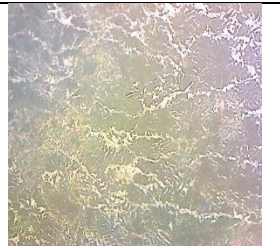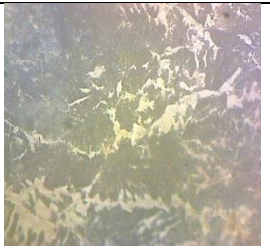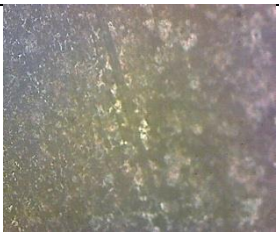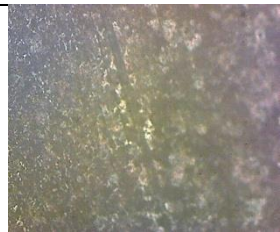

Fig 7.3 photomicrograph of hypo eutectoid steel [22]
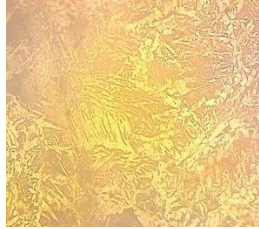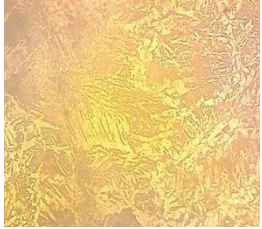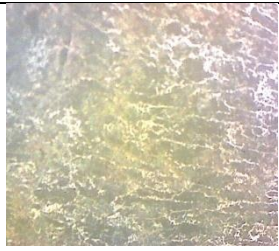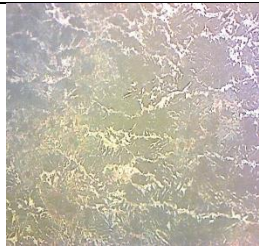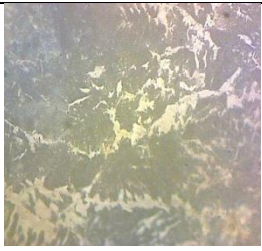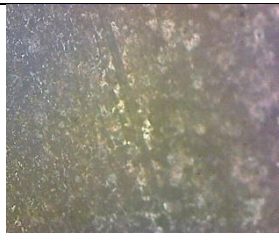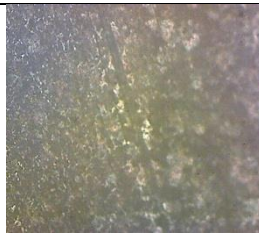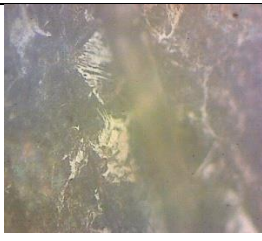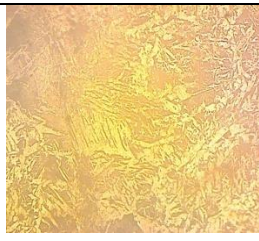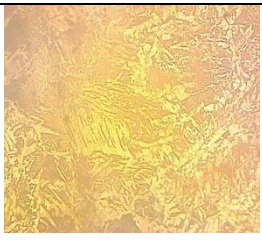
We can see the alternate layers with help of microscope we can also identify the black layer as cementite and white layer as eutectoid ferrite also the thickness of these layers are depends on the cooling rate. The proeutectoid ferrite will disappear at the 0.76% carbon.

7.3 weld bead microstructure

Table 7.1 microstructure at various magnifications

S.NO.	10X zoom	20X zoom	50X zoom
1.			
2.			
3.			
4.			
5.			
6.			

7.			
8.			
9.			
10.			
11.			
12.			
13.			

14.			
15.			
16.			
17.			

The microstructure of the junction between weld bead and heat affected zone is shown in table 7.1. Most learning of weld pool cementing is gotten from the extrapolation of the information of solidifying of castings, ingots, and single precious stones at bring down warm slopes and slower development rates. In this manner, parameters imperative in deciding microstructures in throwing, for example, development rate (R), temperature slope (G), under cooling (δT), and compound structure decide the improvement of microstructures in welds also. Be that as it may, microstructure improvement in the weld zone is more confounded as a result of physical procedures that happen due to the communication of the warmth source with the metal amid welding, including re-melting, heat and liquid stream, vaporization, disintegration of gasses, solidification, ensuing strong state change, stresses, and twisting.

These procedures and their collaborations significantly influence weld pool hardening and microstructure. During welding, where the liquid pool is travelled through the material, the development rate and rate of temperature change fluctuate extensively over the weld pool. Along the fusion line the development rate is low whereas the temperature gradient is 'steepest'. As the weld centreline is drawn nearer, the development rate increments while the temperature slope diminishes. Thus, the microstructure that creates fluctuates significantly from the edge to the centreline of the weld.

In welds, weld pool hardening frequently happens unexpectedly by epitaxial development on the mostly softened grains. Since hardening of the weld metal continues unexpectedly by epitaxial development of the mostly softened grains in the base metal, the weld zone grain structure is fundamentally dictated by the base metal grain structure and the welding conditions. Crystallographic impacts will impact grain development by favouring development along specific crystallographic bearings, to be specific the simple development headings. Conditions for development are ideal when one of the simple development bearings concurs with the warmth stream course. Therefore, among the arbitrarily situated grains in a polycrystalline example, those grains that have one of their simple development crystallographic tomahawks firmly lined up with warm stream heading will develop to the detriment of their neighbouring less positively arranged grains. This is called focused development. Without extra nucleation, this will advance a columnar grain structure.

Chapter 8

CONCLUSIONS AND FUTURE SCOPE

8.1 Conclusions

From the research work following conclusions were drawn:

- After performing the experiments, various outcomes are analysed by using RSM. It has been observed that the bead width increases with the increase of voltage, while the change in other two parameters is less. The increase in %age iron powder increases all three bead geometry parameters but increase in penetration is more than the other two bead parameters. Travel speed is most sensitive parameter to all three bead parameter; but depth of penetration is more sensitive towards travel speed.

- It has also been observed that %age of iron powder, Arc voltage, and welding speed has a significant effect on the residual stress. The welding speed greatly increased the residual stresses over the whole selected input levels (42 – 46 cpm). Whereas, arc voltage has an adverse effect, and the residual stresses value decreased largely at high level (37 Volt).

- F-value of bead width is 595.57, which is more than the reinforcement height, depth of penetration, and residual stress F-value, so we conclude bead width is most important term here.

- The microstructure mainly consists of Ferrite and Pearlite. The microstructure resulting from higher rates of cooling viz. Martensite, upper Bainite, Lower Bainite etc. are not observed, this could be attributed to the covering of weld region by a granulated flux which reduces the heat carried away from the weld zone.

8.2 Future scope:

Every study has a further improvement. Following are the areas which can still be explored in the context of the present research:

- The study had included voltage, velocity and iron powder as the input parameters. Factors like current, multiple wire welding, different size of wire etc. can be incorporated to find out their effects on the bead

geometry features and metallurgy.

- Shape relationships like weld penetration shape factor and weld reinforcement form factor can also be considered along with the bead geometry as outputs in the study.

- Modeling of the SAW process using Neuro Genetic Algorithm, Neuro Differential algorithm etc can be done and their results can be compared with existing models.

- Apart from bead geometry, studies can be undertaken to analyses the effect of process parameters on the mechanical properties of the joint, like Toughness, Ultimate Tensile Strength.

REFERENCES

[1]   Chandel R.S, Seow H.P and Cheong F.L, 1997 "Effect of increasing deposition rate on the bead geometry of submerged arc welds" , Journal of Materials Processing Technology; **72**: 124 – 128.

[2]   Karadeniz E , Ozsarac U, Yildiz C, 2007, "The effect of process parameters on penetration in gas metal arc welding processes" Materials and Design; **28**: 649– 656

[3]   Gunaraj V, Murugan N, 1999, "Application of response surface methodology for predicting weld bead quality in submerged arc welding of pipes". Journal of Material Processing Technology; **88**:266–275.

[4]   Gunaraj V, Murugan N, 1999, "Prediction and comparison of the area of the heat- affected zone for the bead-on-plates and bead-on-joint in submerged arc welding of pipes" Journal of Material Processing and Technology; **95**: 246–261.

[5]   Yang L.J, Bibby M.J, Chandel R.S, 1999, "Linear regression equations for modelling the submerged-arc welding process" Journal of Material Processing and Technology; **39**:33–42

[6]   Srivastav B.K, Tewari S.P, Prakash J, 2010, "A review on effect of arc welding parameters on mechanical behaviour of ferrous metals/alloys" International Journal of Engineering Science and Technology; **2(5)**: 1425-1432

[7]   Benyounis KY, Bettamer AH, Olabi AG, Hashmi MSJ, 2004 "Prediction the impact strength of spiral-welded pipe joints in Submerged arc welding of low carbon steel" In: Proceedings of IMC21, 1–3 September. Limerick; 2004. p. 200– 210Muruganan N, Gunaraj V, 2005, "Prediction and control of weld bead geometry and shape relationships in submerged arc welding of pipes" Journal of Materials Processing Technology; **168** : 478–487

[8]   Koleva E. 2005, "Electron beam weld parameters and thermal efficiency improvement" Vacuum J ; **77** : 413–421

[9]   Benyounis KY, Olabi AG, Hashmi MSJ., 2005, "Effect of laser welding parameters on the heat input and weld-bead profile." Journal of Material Processing

Technology; **164**: 978–985

[10]   Heidarzadeh A , Khodaverdizadeh H, Mahmoudi A, Nazari E , 2012, "Tensile behavior of friction stir welded AA 6061-T4 aluminum alloy joints", Materials and Design; **37**: 166-173

[11]   Andersen K, Cook G.E, Karsai G, Ramaswamy K, 1990, "Artificial neural networks applied to arc welding process modeling and control" IEEE Transactions Industrial Applications.; **26**: pp. 824–830

[12]   Cook G.E**,** Barnett R.J **,** Andersen K, Straw A.M, 1993"Weld Modelling and Control Using Artificial Neural Networks," IEEE, 2181-2189.

[13]   Nagesh D.S, Datta G.L, 2002 "Prediction of weld bead geometry and penetration in shielded metal-arc welding using artificial neural networks" Journal of Material Processing Technology, ; **123** : pp. 303–312

[14]   Pal S, Pal S.K , Samantaray A.K, 2008, "Artificial neural network modeling of weld joint strength prediction of a pulsed metal inert gas welding process using arc signals" Journal of Material Processing Technology; **202**: 464-474

[15]   Cevik A, Kutuk M.A , Erklig A , Guzelbey I.H , 2008 "Neural network modeling of arc spot welding", Journal of Materials Processing Technology; **202**: 137– 144.

[16]   Eroglu M , Aksoy M , Orhan N,1999, "Effect of coarse initial grain size on microstructure and mechanical properties of weld metal and HAZ of a low carbon steel" Material Science and Engineering; **A269**: 59-66

[17]   Kiran D.V, Basu B, De A, 2012, "Influence of process variables on weld bead quality intwo wire tandem submerged arc welding of HSLA steel" Journal of Material Processing Technology, doi:10.1016/j.jmatprotec.2012.05.008

[18]   Gunaraj V, Murugan N, 1999, "Prediction and comparison of the area of the heat-affected zone for the bead-on-plate and bead-on-joint in submerged arc welding of pipes" , Journal of Material Processing Technology; **95** : 246-261

[19]   Kolhe K.P, Datta C.K , 2008, "Prediction of microstructure and mechanical properties of multipass SAW" Journal of Material Processing Technology; 1**97**: 241-249

[20]   Kumar amit, bhardwaj Deepak, 2013 Enrichment of flux by nickel to improve impact strength in submerged arc welding IJCR 5(12):4181-4186 ·

[21]   Benyounis K.Y, Olabi A.G., 2008, "Optimization of different welding processes using statistical and numerical approaches – A reference guide" Advances

in Engineering Software: **39** ; 483–496

[22]   Juang SC, Tarng YS, 2002, "Process parameters selection for optimizing the weld pool geometry in the tungsten inert gas welding of stainless steel." Journal of Material Processing Technology;**122**: 33–37.

[23]   Wang KK, Rasmussen G. 1972. "Optimization of inertia welding process by response surface methodology." Journal of Engineering Industry; **94(4)**:999–1006.

[24]   Koichi O, Hiroshi Y, Seiichi K, Kazuhiko S., 1993 "Optimization of friction welding condition for S4 5C carbon steel using a statistical technique". Journal of Japanese Welding Society; **24(2)**: 47–53.

[25]   Lightfoot MP, Bruce GJ, McPherson NA, Woods K., 2005 "The application of artificial neural networks to weld-induced deformation in ship plate." Weld Journal, AWS and WRC: 23-s–6-s.

[26]   Sterjovski Z, Nolan D, Carpenter KR, Dune DP, Norrish J., 2005 "Artificial neural network for modelling the mechanical properties of steels in various applications." Journal of Material Processing Technology; **170(3)**:336–544.

[27]   Okuyucu H, Kurt A, Arcaklioglu E. 2007 "Artificial neural network application to the friction stir welding of aluminium plates." Journal of Material Design; **29:**78–84

[28]   Wei Y, Bhadeshia HKD, Sourmail T., 2005 "Mechanical property prediction of commercially pure titanium welds with artificial neural network". Journal of Material Science Technology ;**21(3)**: 403–407.

[29]   Canyurt OE., 2005 "Estimation of welded joint strength using genetic algorithm approach. International Journal Mechanical Science; **47**:1249–61.

[30]   Di, L., Srikanthan, T., Chandel, R.S., Katsunori, I., 2001."Neural-network based self-organized fuzzy logic control for arc welding". Engineering Application of Artificial Intelligence; 14: 115–124.

[31]   Indacochea J.E , 1992, "Cr-Mo Steel Welding Metallurgy", Key Engineering Materials; 69-70 : 47-94

[32]   Ma L. W., Wu X. and Xia K., 2008, "Microstructure and property of a medium Carbon steel processed by equal channel angular pressing" , Materials forum ;32

[33]   Linert, T.J., Tellwag Jr., W.L., Grimmett, B.B., Waree, R.W., 2003. Friction stir welding studies on mild steel" Weld Journal; 80: 1-s–9-s.

[34]   McGrath, J.T., et al., 1988. "Microstructural mechanical property relationships in thick section narrow groove welds". Welding Journal. ;67: 196-s–201-s.

[35]   Richard, L., Richard, W., 1994. Economical repair of turbo machinery shaft by SAW." Welding Journal ; 73:, 39–44.

[36]   Wang, W., Liu, S., 2002. "Alloying and microstructural management in developing SMAW electrodes for HSLA-100 steel". Welding Journal;82: 132-s-145-s

[37]   Aslan N, 2008 "Application of response surface methodology and central composite rotatable design for modelling and optimization of a multigravity separator for chromite concentration." Power Technology;185 : 80-86.

[38]   http://arxiv.org/ftp/cs/papers/0308/0308031.pdf

[39]   http://en.wikipedia.org/wiki/Unsupervised_learning

[40]   http://www.statsoft.com/textbook/experimental_design/#centrala   # Introduction to Central Composite Deisgn

[41]   http://en.wikipedia.org/wiki/Central_composite_design

[42]   http://www.doe.soton.ac.uk/elearning/section2.18.jsp

[43]   Davies A.C., Welding Science and technology, Vol-1,Ninth Edition Cambridge university press.

[44]   Montgomery D.C, 2006, " Design and analysis of Experiments" ,Wiley-INDIA edition, New Delhi

[45]   Sindo, K., 2002. "Metallurgy of Welding", second ed. Wiley-Interscience.

[46]   Parmar R.S., 2010, "Welding Process and Technology", Second edition, Khanna Publication.